

# RAID: An In-Training Defense against Attribute Inference Attacks in Recommender Systems

Xiaohua Feng  
fengxiaohua@zju.edu.cn  
Zhejiang University  
Hangzhou, China

Yuyuan Li  
y2li@hdu.edu.cn  
Hangzhou Dianzi University  
Hangzhou, China

Fengyuan Yu  
fengyuanyu@zju.edu.cn  
Zhejiang University  
Hangzhou, China

Ke Xiong  
happywinder@zju.edu.cn  
Zhejiang University  
Hangzhou, China

Junjie Fang  
junjiefang@hdu.edu.cn  
Hangzhou Dianzi University  
Hangzhou, China

Li Zhang  
zhanglizl80@gmail.com  
Zhejiang University  
Hangzhou, China

Tianyu Du  
zjradty@zju.edu.cn  
Zhejiang University  
Hangzhou, China

Chaochao Chen\*  
zjuccc@zju.edu.cn  
Zhejiang University  
Hangzhou, China

## ABSTRACT

In various networks and mobile applications, users are highly susceptible to attribute inference attacks, with particularly prevalent occurrences in recommender systems. Attackers exploit partially exposed user profiles in recommendation models, such as user embeddings, to infer private attributes of target users, such as gender and political views. The goal of defenders is to mitigate the effectiveness of these attacks while maintaining recommendation performance. Most existing defense methods, such as differential privacy and attribute unlearning, focus on post-training settings, which limits their capability of utilizing training data to preserve recommendation performance. Although adversarial training extends defenses to in-training settings, it often struggles with convergence due to unstable training processes. In this paper, we propose RAID, an in-training defense method against attribute inference attacks in recommender systems. In addition to the recommendation objective, we define a defensive objective to ensure that the distribution of protected attributes becomes independent of class labels, making users indistinguishable from attribute inference attacks. Specifically, this defensive objective aims to solve a constrained Wasserstein barycenter problem to identify the centroid distribution that makes the attribute indistinguishable while complying with recommendation performance constraints. To optimize our proposed objective, we use optimal transport to align users with the centroid distribution. We conduct extensive experiments on four real-world datasets to evaluate RAID. The experimental results validate the effectiveness of RAID and demonstrate its significant superiority over existing methods in multiple aspects.

Permission to make digital or hard copies of all or part of this work for personal or classroom use is granted without fee provided that copies are not made or distributed for profit or commercial advantage and that copies bear this notice and the full citation on the first page. Copyrights for components of this work owned by others than the author(s) must be honored. Abstracting with credit is permitted. To copy otherwise, or republish, to post on servers or to redistribute to lists, requires prior specific permission and/or a fee. Request permissions from [permissions@acm.org](mailto:permissions@acm.org).  
*Conference acronym 'XX, June 03–05, 2018, Woodstock, NY*

© 2018 Copyright held by the owner/author(s). Publication rights licensed to ACM.  
ACM ISBN 978-1-4503-XXXX-X/2018/06...\$15.00  
<https://doi.org/XXXXXXXX.XXXXXXX>

## CCS CONCEPTS

• Information systems → Collaborative filtering; • Security and privacy → Human and societal aspects of security and privacy.

## KEYWORDS

Recommender System, Collaborative Filtering, Attribute Inference Attack

## ACM Reference Format:

Xiaohua Feng, Yuyuan Li, Fengyuan Yu, Ke Xiong, Junjie Fang, Li Zhang, Tianyu Du, and Chaochao Chen. 2018. RAID: An In-Training Defense against Attribute Inference Attacks in Recommender Systems. In *Proceedings of Make sure to enter the correct conference title from your rights confirmation email (Conference acronym 'XX)*. ACM, New York, NY, USA, 18 pages. <https://doi.org/XXXXXXXX.XXXXXXX>

## 1 INTRODUCTION

Attribute Inference Attacks (AIA) pose emerging threats to user privacy across various application domains, ranging from recommender systems [49, 55, 56], to social media [9, 20, 21, 61] and mobile platforms [43, 48]. In such attacks, adversaries exploit exposed user profiles to infer private attributes, including location, gender, sexual orientation, and political views. For instance, in recommender systems, the exposed profile could be a list of items rated by users, such as movies, mobile applications, and videos [19, 52, 55]. In social media, it might be the list of pages a user has liked on a social platform [37]. Attacks can utilize this profile to precisely infer sensitive attributes, leading to privacy leakages. Notably, recommender systems rely heavily on sensitive interactions and contextual data to enhance the performance of recommendations. Particularly for new users (i.e., cold-start), recommender systems extensively integrate side information about users [1, 54, 59]. These factors further increase the risk of AIA for recommender systems in real-world scenarios. Additionally, given that models in recommender systems nearly span those common models in social media and mobile platforms, defensive strategies against AIA developed for recommender

systems can be easily extended to other domains. For example, incorporating Differential Privacy (DP) techniques into recommendation systems to protect users' privacy attributes can also be applied to social media platforms, thereby reducing the success rate of AIA. Based on the analysis above, we focus on exploring AIA within recommender systems in this paper.

Recommender systems, as effective solutions for combating information overload, have been widely adopted across various applications [5, 34, 50]. These systems, through machine learning models, can automate the mining of user preferences and their relationships with interaction items. Due to its simplicity and effectiveness, Collaborative Filtering (CF) [35, 51] is the predominant model used in recommender systems. CF encodes user and item embeddings, thereby recommending similar items to users with similar behaviors. Due to the correlation between user-item interactions and private user attributes [29], recommendation models may inadvertently encode sensitive information in their latent embeddings, even though the training data of recommendation models do not explicitly contain information about these private attributes. Existing studies [6, 23, 55] show that if malicious attackers can access the parameters of the recommendation model or its recommendation results, they can accurately infer private user attributes.

In response to AIA on recommender systems, existing studies propose various defense methods. The primary goal of these methods is to effectively defend against AIA while ensuring that the recommendation performance remains unaffected. The main defense methods include techniques based on DP [4, 40, 62], attribute unlearning [23, 39], and adversarial training [6, 16]. The DP methods employ a Post-Training (PoT) setting, introducing dynamic perturbations into the model's embeddings to reduce the probability of successful attacks [62]. Similarly, attribute unlearning methods also adopt the PoT setting [39]. After model training is completed, attribute unlearning protects private attributes by minimizing the differences between embeddings. However, existing methods have three main issues: *Issue 1. Insufficient recommendation preservation*. As shown in Figure 1, due to limited accessibility, PoT approaches cannot directly utilize training data, leading to a noticeable decline in the model's recommendation performance; *Issue 2. Lack of theoretical guarantees*. Existing methods are based on intuition guidance, lacking a theoretical guarantee of defense; and *Issue 3. Instability of adversarial training*. Although the adversarial training methods extend defense from PoT to In-Training (InT) settings, the instability of the optimization process makes it difficult to ensure convergence.

**Our work.** To address these issues, we propose a privacy-preserving recommender system named RAID (Recommendation Attribute Inference Defender). Regarding *Issue 1*, we extend the defense method to the InT setting, thereby fully utilizing the training data to better preserve recommendation performance. In other words, we can fine-tune the model with the original recommendation objective using training data. Regarding *Issue 2*, we define a defensive objective based on the principle that the predictive performance of a classification model (i.e., attacker) on distribution-consistent data is equivalent to random prediction. This means the objective is to minimize the discrepancy among different attribute distributions, consolidating them into a single consistent distribution. To achieve this, we introduce the Wasserstein distance [18] as a

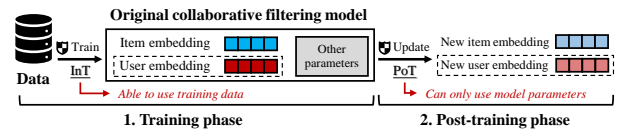


**Figure 1: The difference between the settings of In-Training (InT) and Post-Training (PoT) primarily lies in their implementation stages and dependency on data. The InT setting is implemented during the model training phase, allowing it to protect user attributes while utilizing the original training data to preserve recommendation performance. In contrast, the PoT setting is implemented after the model training is completed, at which point only the model's parameters are accessible [39]. The experimental results of the comparison are reported in Section 6.1.**

measure of distribution discrepancy, transforming the AIA defense problem into one where all attribute distributions converge toward a centroid distribution. Our proposed approach provides theoretical guarantees for AIA defense from the perspective of the attacker. Regarding *Issue 3*, we separate the original recommendation objective training with the computation of the centroid distribution (i.e., our proposed additional defensive objective) to ensure more stable optimization. To alleviate potential conflicts between the two objectives, we further impose a recommendation constraint on the centroid distribution, which smooths the optimization trajectory. Additionally, due to the high computational complexity associated with calculating the centroid distribution, we opt to update it at intervals rather than after every training iteration.

The main contributions of this paper are:

- We explore defenses against AIA in recommender systems and propose a novel method named RAID. Our proposed method improves upon traditional attribute unlearning methods and extends them to the InT setting, effectively protecting users' private attributes while preserving recommendation performance.
- In addition to the original recommendation objective, we define the defense objective against AIA as minimizing the discrepancy in distributions under different attributes. This definition ensures that the training data obtained by the attacker follows a single consistent distribution, thereby rendering the predictive performance of attackers trained on such data equivalent to random prediction.
- To ensure stability in the training process and improve training efficiency, we separate the recommendation objective training from the computation of constraint centroid distribution, updating the centroid distribution at regular intervals.
- We conduct extensive experiments and in-depth analyses across mainstream recommendation models on real-world datasets, to evaluate our proposed method w.r.t. privacy protection and recommendation performance.

## 2 RELATED WORK

### 2.1 Recommender Systems

Recommender systems analyze user-item interactions and other side information to rank items based on user preferences. Among

the multitude of recommendation models, CF has been widely applied in practical settings. The concept of CF is recommending similar items to users with similar behaviors [35, 51]. In CF, let  $\mathcal{U}$  and  $\mathcal{V}$  represent the sets of users and items, respectively, and  $\mathcal{R}$  denotes the user-item interaction behavior matrix. The primary objective is to learn the user embedding matrix  $P$  and the item embedding matrix  $Q$ . In the existing literature [33], CF can be categorized into three types: i) **Matrix Factorization-based CF** [45], which decomposes the user-item interaction matrix  $\mathcal{R}$  into the product of two low-dimensional matrices,  $P$  and  $Q$ . The product of these two matrices generates a full-ranking matrix to predict the interactions between all users and items; ii) **Neural Network-based CF** [27], which encodes each user or item into a latent vector space; and iii) **Graph-based CF** [26], which considers the user-item interactions from the perspective of a user-item interaction graph. Here, a user’s interaction history is akin to the user’s first-order connections, and embeddings of users and items are learned on the graph network. Regardless of the approach used, the primary objective of CF is to learn embeddings for users and items. Thus, our defensive method operates on these embeddings, making it adaptable to most recommendation models.

## 2.2 Attribute Inference Attacks

Recent research demonstrates that users are highly vulnerable to AIA [9, 14, 15, 20, 21, 43, 48, 49, 55, 56, 60, 61]. In such attacks, the attacker acquires a dataset related to the target user, referred to as user profiles, to infer the user’s private attributes, such as gender, location, political views, or sexual orientation. Specifically, the attacker employs a machine learning classifier, inputting the user profiles to predict the user’s attribute values. This classifier is trained on a shadow dataset containing user profiles alongside corresponding attribute values. Such attacks are extensively explored in the following three types of scenarios.

**Scenario I.** In recommender systems, a user’s user profiles might consist of their ratings for certain items. Previous study [55] verifies that attackers can use a logistic regression classifier to predict a user’s gender based on their ratings of movies. Subsequent studies [28, 41] replace the classifier with more effective Multilayer Perceptrons (MLP) to achieve improved results. **Scenario II.** In social media contexts [9, 20, 21, 61], attackers can similarly use machine learning classifiers to infer target users’ private attributes based on their user profiles on social media, such as pages liked or shared, music playlists, and friends lists. The attack pattern in social media closely mirrors that in recommender systems. **Scenario III.** In mobile applications, a previous study [43] demonstrates attackers could use classifiers to infer a user’s location based on the total power consumption of the user’s smartphone.

The attack patterns across these three scenarios are strikingly similar, with attackers collecting datasets from users who have disclosed their attributes and using this data as a shadow dataset to train classifiers. Our defensive methods against AIA in recommender systems described in this paper can be readily extended to other scenarios.

## 2.3 AIA Defenses

To defend against AIA, researchers propose privacy-preserving methods based on various strategies, generally categorized into three types: DP-based methods, attribute unlearning methods, and adversarial training methods.

- **DP.** DP aims to add noise to user profiles to prevent an attacker’s classifier from accurately inferring users’ private attributes [4, 62]. Since additional noise must be introduced into the training data or model parameters, DP methods may reduce the utility of the model [29].
- **Attribute unlearning.** In recommender systems, attribute unlearning methods aim to make the model unlearn certain private attributes of users by training the model under the PoT setting. Specifically, by reducing the distances between sample embeddings during the PoT process, it becomes challenging for attackers to effectively classify the data [39]. However, since PoT adjustments cannot utilize the original recommendation data, this may significantly reduce the model’s recommendation performance.
- **Adversarial training.** Existing research views attackers and recommender systems as adversarial parties, implementing defenses by solving a min-max problem. Specifically, Beigi et al. introduce a minimax game between Bayesian personalized ranking and worst-case attackers, where user representations can be combined with interaction data to recover sensitive user information [6]. Ganhoor et al. integrate this approach into a VAE-based recommendation model to remove private information from latent variables [16]. Although these adversarial training methods are computationally feasible, their training process remains unstable, and they cannot guarantee theoretical privacy protection.

## 3 PRELIMINARY

To enhance readability, we briefly introduce the notation used in this paper, followed by a succinct overview of the Wasserstein distance and the threat model.

### 3.1 Notations

*Definition of recommendation.* CF involves encoding users and items into embeddings and optimizing these embeddings by minimizing loss functions. Let  $\mathcal{U} = \{u_1, \dots, u_N\}$  and  $\mathcal{V} = \{v_1, \dots, v_M\}$  respectively represent sets of users and items, with  $N$  and  $M$  denoting the numbers of users and items, respectively. The user-item interaction matrix  $\mathcal{R} \in \mathbb{R}^{N \times M}$  denotes the interaction records between each user and item. In this paper, we adopt the implicit feedback setting where the element of interaction matrix  $r_{u,v} = 1$  if there is an interaction between user  $u$  and item  $v$  else  $r_{u,v} = 0$ . Generally, many existing CF approaches utilize encoder networks  $f(\cdot)$  to generate embeddings of users and items  $f(u), f(v) \in \mathbb{R}^d$ .

*Definition of defense.* Let  $\mathcal{D} = \{(u_n, y_n, a_n)\}_{n=1}^N$  as a set of  $N$  independent and identically distributed (i.i.d.) samples drawn from an unknown probability distribution over  $\mathcal{U} \times \mathcal{Y} \times \mathcal{A}$ , where  $u_n$  denotes the  $n$ -th user, with  $y_n = f(u_n)$  denotes user embeddings, and  $a_n$  represents private attributes. Each sample point  $(u_n, y_n, a_n)$  corresponds to a user profile record. Given the number attribute classes  $K$ , we denote  $\mathcal{D}^i = \{(u_n, y_n, a_n) \in \mathcal{D}, s.t. a_n = a^i, i \in [1, 2, \dots, K]\}$  as the set of users have the attribute  $a^i$ , where  $a^i$  represents the  $i$ -th

category of attribute  $a$ . The number of users in this set is denoted as  $|\mathcal{D}^i| = N^i$ , and  $y_n \in \mathcal{D}^i$  is also denoted as  $y_n^i$ . Note that this paper focuses on protecting a single privacy attribute, with one defensive objective corresponding to each attribute. The term “attribute distribution” refers to the embedding distribution of users with the same class label in the target attribute. The target attribute is the one to unlearn, and attribute labels denote specific categories (e.g., “male” or “female”). Depending on the context, we use either “class distribution” or “attribute distribution”, but they refer to the same concept in this paper. Additionally, while users may have multiple privacy attributes that require protection, our proposed framework can be readily adapted to protect multiple attributes simultaneously by incorporating multiple defensive objectives. Let  $U$ ,  $Y$ , and  $A$  be random variables corresponding to  $x$ ,  $u$ , and  $a$  respectively, each having a probability density function  $p(\cdot)$ . Thus, define  $Y^i$  as the random variable relative to set  $\mathcal{D}^i$ , we have the probability density function  $p(Y^i) = p(Y | A = a^i)$ .

### 3.2 Wasserstein Distance

In this paper, we employ Wasserstein distance [18] as the distance measurement between distributions in subsequent derivations. To enhance the readability, we briefly introduce its definition in this section.

Given two probability measures  $\alpha$  and  $\beta$  on spaces  $\mathcal{X}$  and  $\mathcal{Y}$  respectively, each endowed with densities  $p_X$  and  $p_Y$  (i.e.,  $d\alpha(x) = p_X(x)dx$  and  $d\beta(y) = p_Y(y)dy$ ), consider a transportation map  $T : \mathcal{X} \rightarrow \mathcal{Y}$  that for any measurable subset  $\mathcal{B} \in \mathcal{Y}$  satisfies  $\int_{\mathcal{B}} p_Y(y)dy = \int_{T^{-1}(\mathcal{B})} p_X(x)dx$  (mass conservation constraint). This means that the mass of the measurable subset  $\mathcal{B}$  w.r.t. the density  $p_Y$  is equal to the mass of the set  $T^{-1}(\mathcal{B})$  w.r.t. the density  $p_X$ . Let  $\mathcal{T}$  be the set of all transportation maps from  $\mathcal{X}$  to  $\mathcal{Y}$ , and let  $c : \mathcal{X} \times \mathcal{Y} \rightarrow [0, +\infty]$  be a cost function where  $c(x, T(x))$  represents the cost of transporting  $x$  to  $T(x)$ . In the original formulation [46], the optimal transportation map  $T$  is the map that minimizes the total transportation cost:

$$\min_T \left\{ \int_{\mathcal{X}} c(x, T(x))d\alpha(x) : T_{\#}\alpha = \beta \right\}, \quad (1)$$

where  $T_{\#}$  represents the push-forward operator that satisfies the mass conservation constraint when mapping the probability measure  $\alpha$  onto  $\beta$ .

Given the non-convex nature of the feasible set in the aforementioned problem, Kantorovich [31] reformulates the optimal transport problem by finding the optimal joint distribution in the set of joint distributions on  $\mathcal{X} \times \mathcal{Y}$ , denoted as

$$\min_T \left\{ \int_{\mathcal{X} \times \mathcal{Y}} c(x, y)dT(x, y) : P_{X\#}T = \alpha, P_{Y\#}T = \beta \right\}, \quad (2)$$

where  $P_{X\#}$  and  $P_{Y\#}$  are the push-forward operators of the projection  $P_X(x, y) = x$  and  $P_Y(x, y) = y$ , which map the joint distribution to the respective marginal distributions. Additionally,  $T$  has a density  $p_{X \times Y}$  such that  $dT(x, y) = p_{X \times Y} dx dy$ . This reformulation allows the problem to be addressed within a convex framework, facilitating the application of linear programming techniques to find solutions that minimize the transportation cost across the distributions.

Assuming that  $\mathcal{X} = \mathcal{Y}$  and for some  $p \geq 1$  such that  $c(x, y) = d(x, y)^p$ , where  $d(x, y)$  is the distance on space  $\mathcal{X}$ , the  $p$ -Wasserstein distance is defined as

$$\mathcal{W}_p(\alpha, \beta) = \min_T \left( \int_{\mathcal{X} \times \mathcal{Y}} c(x, y)dT(x, y) \right)^{\frac{1}{p}}, \quad (3)$$

where  $T$  must satisfy the same constraints in Eq. (2).  $\mathcal{W}_p$  is symmetric and positive,  $\mathcal{W}_p(\alpha, \beta) = 0$  if and only if  $\alpha = \beta$ , and it satisfies the triangle inequality

$$\forall \alpha, \beta, \gamma \in \mathcal{S}, \mathcal{W}_p(\alpha, \beta) \leq \mathcal{W}_p(\alpha, \gamma) + \mathcal{W}_p(\gamma, \beta), \quad (4)$$

where  $\mathcal{S}$  is the space containing  $\alpha$ ,  $\beta$ , and  $\gamma$ .

### 3.3 Threat Model

*Adversary’s goal.* The goal of the attacker is to infer users’ sensitive attributes from available information. In this paper, we focus on discrete attributes with two or more labels. Assuming the information possessed by the attacker can be represented as  $I = \{(y_n, a_n)\}_{n=1}^{\tilde{N}}$ , where  $\tilde{N} < N$  denotes the number of users with available attributes leaked to the attacker. The attacker aims to train a classifier  $\vartheta(\cdot) : \mathbb{R}^d \rightarrow \{1, 2, \dots, K\}$ .

*Adversary’s knowledge.* In recommender systems, the knowledge relied upon by AIA can generally be categorized into two types: *i) Model parameters.* Existing research [16, 39] indicates that basic machine learning models, due to their representative learning capabilities, can successfully infer user attributes from user embeddings learned through CF models. *ii) Recommendation results.* Furthermore, personalized recommendation results can also be exploited by attackers, as they significantly reflect user preferences and attribute information [55]. Following prior studies [16, 39], we assume a gray-box scenario where attackers access partial model parameters, i.e., user embeddings. The adversary is able to access an IID shadow dataset of available information above.

## 4 METHOD

In this section, we introduce our proposed privacy-preserving recommender system, RAID. An overview of RAID is shown in Figure 2. We first introduce the definitions of both the recommendation and defensive objectives, then present the training algorithm that integrates these two objectives.

### 4.1 In-training for Recommendation

*Recommendation objective.* The recommendation model acquires embeddings for users and items, and performs recommendation tasks by utilizing the similarity (e.g., vector dot product) between user and item embeddings. As described in Section 3.1, most CF models learn embeddings for users and items through an encoder network  $f(\cdot)$ . For instance, neural network-based models typically employ neural network layers as encoders, while graph-based models incorporate neighborhood information into the encoder.

To preserve recommendation performance, RAID is constructed under InT setting, allowing the use of model’s training data to enhance recommendation performance. Specifically, following prior work [27], we adopt the widely-used Cross-Entropy (CE) loss as

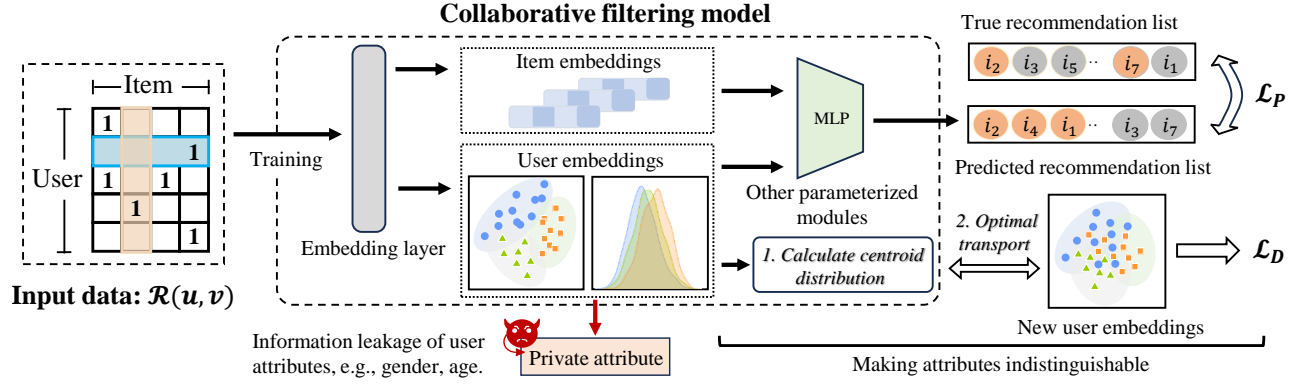


Figure 2: RAID, established under the InT setting, can directly use the original training data to preserve recommendation performance. Additionally, RAID defines a defensive objective to ensure that the class distribution of protected attributes is independent of class labels, which is equivalent to making all class distributions indistinguishable. Based on this, RAID first calculates a centroid distribution that satisfies the constraints on recommendation performance and then uses optimal transport to align all class distributions with it, rendering the class distributions indistinguishable.

the recommendation objective:

$$\mathcal{L}_P = \frac{\sum_{(u,v) \in \mathcal{R} \cup \mathcal{R}^-} \log \left( (s_{u,v})^{r_{u,v}} (1 - s_{u,v})^{(1-r_{u,v})} \right)}{|\mathcal{R} \cup \mathcal{R}^-|}, \quad (5)$$

where  $\mathcal{R}^- = \{(u, v^-)\}$  represents the set of uninteracted negative samples, and  $s_{u,v}$  denotes the predicted rating of interaction  $(u, v)$ . For all recommendation models described in this paper, we employ the CE loss during training.

## 4.2 Defending Against AIA

*Defensive objective.* Since the attacker is trained on the user embedding by the recommendation model, defenders (i.e., from the perspective of recommender systems) can intervene in the attacker’s training dataset (i.e., user embeddings) to degrade the effectiveness of the classifier model trained by the attacker. Given that the attacker is typically unknown, the defense strategy proposed in this paper is based on the attacker’s training dataset. Specifically, the defender’s objective can be expressed as

$$\mathcal{P}(Y | A = a^i) = \mathcal{P}(Y | A = a^j), \quad \forall i \neq j, a^i, a^j \in \mathcal{A}. \quad (6)$$

This indicates that the user embeddings obtained under different classes by the attacker have the same distribution, implying a minimal correlation between the training data and private user attributes. Consequently, a classifier trained on such data will perform no better than random prediction.

Let  $\mathcal{P}(Y^i) = \mathcal{P}(Y | A = a^i)$ . In order to achieve the target expressed in Eq. (6), we minimize the following loss function:

$$\mathcal{L}_D(\theta) = \min_{\theta} \sum_{i=1}^K \sum_{j=1, j \neq i}^K Dis(\mathcal{P}(Y^i), \mathcal{P}(Y^j)), \quad (7)$$

where  $\mathcal{P}(Y^i)$  denotes the output distribution for the  $i$ -th category and  $Dis(\cdot, \cdot)$  represents the distance between two distributions. In this paper, we employ the squared 2-Wasserstein distance ( $\mathcal{W}_2$

distance) to measure the distance between distributions. The motivation for using the  $\mathcal{W}_2$  distance lies in its well-defined and computable nature, even between distributions with non-overlapping supports. Consequently, Eq. (7) can be reformulated as follows:

$$\mathcal{L}_D(\theta) = \min_{\theta} \sum_{i=1}^K \sum_{j=1, j \neq i}^K \mathcal{W}_2^2(\mathcal{P}(Y^i), \mathcal{P}(Y^j)). \quad (8)$$

Given that the Wasserstein distance satisfies the triangle inequality (4), it yields an upper bound for Eq. (8):

$$\begin{aligned} \mathcal{L}_D(\theta) &\leq \min_{\theta} \sum_{i=1}^K \sum_{j=1, j \neq i}^K [\mathcal{W}_2(\mathcal{P}(Y^i), \mathcal{P}^*) + \mathcal{W}_2(\mathcal{P}(Y^j), \mathcal{P}^*)]^2 \\ &\leq \min_{\theta} \sum_{i=1}^K \sum_{j=1, j \neq i}^K 2 [\mathcal{W}_2^2(\mathcal{P}(Y^i), \mathcal{P}^*) + \mathcal{W}_2^2(\mathcal{P}(Y^j), \mathcal{P}^*)] \\ &= \min_{\theta} 4(K-1) \sum_{i=1}^K \mathcal{W}_2^2(\mathcal{P}(Y^i), \mathcal{P}^*), \end{aligned} \quad (9)$$

where  $\mathcal{P}^*$  is an unknown distribution located in the same space as  $\mathcal{P}(Y^i)$ . Upon obtaining  $\mathcal{P}^*$ , Eq. (9) can be directly optimized using gradient descent, a process equivalent to making all output distributions  $\{\mathcal{P}(Y^i)\}$  converge towards  $\mathcal{P}^*$ . Therefore, based on this upper bound, we can minimize Eq. (8) by minimizing Eq. (9).

*Restrictions on Distribution  $\mathcal{P}^*$ .* Although aligning each class distribution closely with distribution  $\mathcal{P}^*$  can achieve the goal of defense, not every distribution  $\mathcal{P}^*$  is suitable for preserving recommendation performance. Thus, we set the following two constraints on distribution  $\mathcal{P}^*$ :

- *Constraint 1.* According to [24], to minimize the impact on recommendation performance, class distributions with a larger number of samples should be adjusted less, i.e., be closer to  $\mathcal{P}^*$ , while those with fewer samples should be adjusted more, i.e., be further from  $\mathcal{P}^*$ .

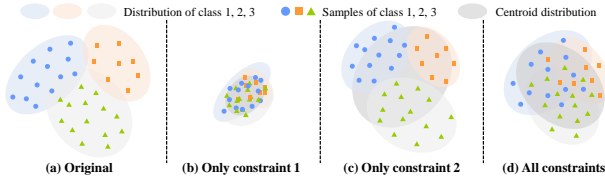


**Figure 3: The function of each constraint. (a) In the initial stage, distinct decision boundaries between class distributions provide potential attacking foundations. (b) When Constraint 1 is applied, distributions are correctly centered but too compact, leading to significant overlap among user embeddings and reducing their ability to distinguish information beyond protected attributes. (c) When Constraint 2 is applied, the centroids become overly relaxed and unstable, causing only slight movements of each class distribution. There remains a clear decision boundary between the class distributions.**

- *Constraint 2.* Distribution  $\mathcal{P}^*$  should not be overly compact. If  $\mathcal{P}^*$  is too compact, user embeddings may collapse to this overly compact distribution, not only losing the information of the protected attributes but also potentially losing other important information.

To more clearly convey our ideas, we illustrate the role of each constraint in Figure 3. To provide a formalized representation, we first define the differential entropy:

$$H(\mathcal{P}) := - \int_X \log \left( \frac{d\mathcal{P}}{dx} \right) d\mathcal{P}(x), \quad (10)$$

where a smaller  $H(\mathcal{P})$  implies that the distribution  $\mathcal{P}$  is more compact. Subsequently, these two constraints can be expressed as

$$\mathcal{P}^* = \arg \min_{\mathcal{P}} \underbrace{\sum_{i=1}^K \lambda_i \mathcal{W}_2^2(\mathcal{P}(Y^i), \mathcal{P})}_{\text{Constraint 1}} \underbrace{-\tau H(\mathcal{P})}_{\text{Constraint 2}}, \quad (11)$$

where  $\lambda_i$  represents the weight of class distribution  $\mathcal{P}(Y^i)$ , equivalent to the size-normalized summation [2], and  $\tau \geq 0$  is a penalty coefficient used to control the preference for the entropy penalty term  $-H(\mathcal{P})$ .  $\mathcal{P}^*$  is called penalized 2-Wasserstein barycenter.

*Empirical computation.* In practice, since constructing the centroid from the overall distribution  $\{\mathcal{P}(Y^i)\}$  is infeasible, we empirically compute the centroid distribution  $\mathcal{P}^*$  using the empirical distribution  $\hat{\mathcal{P}}(Y^i)$  obtained from  $\mathcal{D}^i$ . Following [30, 32], if the samples in  $\mathcal{D}$  are i.i.d., as  $|\mathcal{D}| \rightarrow \infty$ , with  $\mathcal{W}_2^2(\mathcal{P}(Y^i), \mathcal{P}^*) < \infty$  for all  $i \in [1, 2, \dots, K]$ , the empirical barycenter distribution with penalty term satisfies  $\lim_{\sum_{i=1}^K \mathcal{W}_2^2(\hat{\mathcal{P}}(Y^i), \hat{\mathcal{P}}^*) \rightarrow \sum_{i=1}^K \mathcal{W}_2^2(\mathcal{P}(Y^i), \mathcal{P}^*)}$  almost surely. Subsequently, all computations related to the distribution can be executed empirically.

### 4.3 Putting Together

This section puts together our proposed objectives and formally introduces our RAID framework along with the corresponding computational implementation.

*Overview of RAID.* We define the total loss function over dataset  $\mathcal{D} = \{(u_n, y_n, a_n)\}_{n=1}^{\hat{N}}$  as

$$\mathcal{L}_{ALL}(\theta) = \mathcal{L}_P(\theta) + \eta \sum_{i=1}^K \mathcal{W}_2^2(\hat{\mathcal{P}}(Y^i), \hat{\mathcal{P}}^*), \quad (12)$$

where  $\eta$  is an adjustable coefficient and the last term is the loss of defensive objective  $\mathcal{L}_D(\theta)$ . These two terms represent the losses of recommendation objective and defensive objective, respectively. However, in the initial stage of training, the user embeddings do not adequately reflect their category characteristics, meaning that the centroid distribution computed at this time lacks significance, thus rendering the latter term of the equation less effective. Therefore, RAID adopts a two-phase training strategy:

- **Phase I.** In the initial stage, we only optimize the first term of Eq. (12) to ensure recommendation performance.
- **Phase II.** Once the model achieves preliminary fitting, we optimize the entire equation. Given that the latter term cannot be directly calculated, it must be approached in two steps: *Step 1.* Calculating the empirical centroid distribution  $\mathcal{P}^*$ ; *Step 2.* Treating it as a constant independent of model parameters, and optimizing the entire Eq. (12) using gradient descent.

*Computational implementation.* Since the loss term in Phase I equals the original recommendation model training, we focus on addressing the computational issues in Phase II, which are divided into two steps.

For *step 1*, we utilize following Lemma 1 to compute the empirical barycenter  $\hat{\mathcal{P}}^*$  on  $\{\tilde{y}_q\}_{q=1}^{\hat{N}}$ , where  $\{\tilde{y}_q\}_{q=1}^{\hat{N}}$  represents the atoms (support set) of the centroid distribution  $\hat{\mathcal{P}}^*$ , where  $\delta_y$  is the Dirac distribution at  $y$ . The empirical Wasserstein barycenter can be estimated by  $\hat{\mathcal{P}}^* = \sum_{n=1}^{\hat{N}} \alpha_n \delta_{\tilde{y}_n}$ ,  $\sum_{n=1}^{\hat{N}} \alpha_n = 1$ .

**LEMMA 1.** Given sample-based empirical distributions  $\hat{\mathcal{P}}(Y^i) = \frac{1}{N_i} \sum_{n=1}^{N_i} \delta_{y_n^i}$ ,  $i \in [K]$ , the dual problem of penalized Wasserstein barycenter can be formulated as

$$\max_{g_1, \dots, g_K} \sum_{i=1}^K \lambda_i \sum_{n=1}^{N_i} g_i^c(y_n^i) - \tau \log \sum_{n=1}^{\hat{N}} \exp \left( -\frac{1}{\tau} \sum_{i=1}^K \lambda_i g_i(\tilde{y}_n) \right), \quad (13)$$

where  $g(\cdot)$  denotes the dual problem and  $g_i^c(y_n^i)$  is defined by

$$\min_{p=1, \dots, \hat{N}} \{ \|y_n^i - \tilde{y}_p\|^2 - g_i(\tilde{y}_p) \}.$$

Moreover, Eq. (13) is concave and L-Lipschitz continuous with respect to  $g_i$ 's. If  $(g_i)_{i=1}^K$  solves the dual problem, then  $(g_i^c, g_i)_{i=1}^K$  can be utilized to recover the empirical Wasserstein barycenter  $\hat{\mathcal{P}}^*$  and the optimal couplings  $\{T_i^*\}_{i=1}^K$ .

**PROOF.** The proof is given in Appendix A.  $\square$

For *step 2*, to compute the gradient of Eq. (12), it is necessary to solve for the optimal coupling  $T_i^*$  between each class distribution  $\hat{\mathcal{P}}(Y^i)$  and the centroid distribution  $\hat{\mathcal{P}}^*$ . Since we have computed  $\mathcal{P}^*$  and  $\{\tilde{y}_n\}_{n=1}^{\hat{N}}$ . The calculation of the optimal coupling family  $\{T_i^*\}$  can be solved by iterative KL-projection method [7]. Based on the optimal coupling  $\{T_i^*\}$ , the gradient of Eq. (12) w.r.t.  $\theta$  can be further derived by the following Lemma:

**Algorithm 1** RAID Framework

---

```

1: Inputs: Dataset  $\mathcal{D} = \{(u_n, y_n, a_n)\}_{n=1}^N$ , adjustable coefficients
 $\eta$ , update step size  $\mu$ , optimization rounds  $E^1$  of Phase I, opti-
mization rounds  $E^2$  of Phase II, frequency of barycenter distri-
bution computation  $\xi$ .
2: Initialize: Model parameters  $\theta_0$ .
3: for  $i = 1$  to  $E^1$  do                                     ▶ Phase I
4:   Compute gradients  $\nabla \mathcal{L}_P(\theta)$ .
5:   Update parameters  $\theta_i = \theta_{i-1} - \mu \nabla \mathcal{L}_P(\theta)$ .
6: end for
7: for  $i = E^1 + 1$  to  $(E^1 + E^2)$  do                       ▶ Phase II
8:   if  $((i - E^1) \bmod \xi) == 0$  then
9:     Compute the empirical barycenter distribution  $\hat{\mathcal{P}}^*$ 
       with penalty term and support set  $\{\bar{y}_n\}_{n=1}^{\bar{N}}$  as
       defined in Lemma 1.
10:   end if
11:   Compute gradients  $\nabla \mathcal{L}_D(\theta)$  as defined in Lemma 2.
12:   Update parameters  $\theta_i = \theta_{i-1} - \mu \nabla \mathcal{L}_{ALL}(\theta)$ .
13: end for
14: return  $\theta_{E^1+E^2}$ .

```

---

LEMMA 2. Assuming datasets  $\{y_p^i\}_{p=1}^{N^i}$  and  $\{\bar{y}_q\}_{q=1}^{\bar{N}}$  correspond to empirical distributions  $\hat{\mathcal{P}}(Y^i)$  and  $\hat{\mathcal{P}}^*$  respectively, both distributions  $\hat{\mathcal{P}}(Y^i)$  and  $\hat{\mathcal{P}}^*$  exist within the same space  $\mathcal{S} = \mathbb{R}^d$ . If  $c(y_p^i, \bar{y}_q) = \|y_p^i - \bar{y}_q\|^2$ , we can derive the gradient of  $\mathcal{L}_D(\theta)$  satisfies:

$$\nabla_{\theta} \mathcal{L}_D(\theta) = 2 \sum_{i=1}^K \sum_{p=1}^{N^i} \left[ \partial y_p^i(\theta) \right]^{\top} \left( \frac{y_p^i}{N^i} - \sum_{q=1}^{\bar{N}} T_i^*(p, q) \bar{y}_q \right)_{p=1}^{N^i},$$

where  $\partial y_p^i(\theta) \in \mathbb{R}^{\dim(\theta) \times (N^i d)}$  is the Jacobian of the map  $y_p^i(\theta)$  and  $T_i^*(p, q) = T_i^*(y_p^i, \bar{y}_q)$  represents the transfer amount from  $y_p^i$  to  $\bar{y}_q$  in the optimal coupling matrix  $T_i^*$ .

PROOF. The proof is given in Appendix A.  $\square$

Since the gradient of loss  $\mathcal{L}_P(\theta)$  can be directly computed, based on Lemma 2, the gradient for Eq. (12) can be determined with  $\nabla_{\theta} \mathcal{L}_{ALL}(\theta) = \nabla_{\theta} \mathcal{L}_P(\theta) + \eta \nabla_{\theta} \mathcal{L}_D(\theta)$ . Subsequent updates of parameters adhere to  $\theta_{t+1} = \theta_t - \mu \nabla_{\theta} \mathcal{L}_{ALL}(\theta)$ , where  $\mu$  represents the step size. According to previous studies [10, 12, 30], under the condition of optimal coupling  $T_i^*$  being sparse, the computation of  $\nabla_{\theta} \mathcal{L}_D(\theta)$  can be completed in linear time. However, it is important to note that calculating the centroid distribution  $\hat{\mathcal{P}}^*$  entails a significant computational cost. Therefore, we do not compute it at every step; instead, we opt to perform this calculation every  $\xi$  step, where  $\xi$  is dynamically adjusted based on the progress of training. For a detailed description of the algorithmic process, please refer to Algorithm 1.

## 5 EVALUATION

In this section, we evaluate RAID across four real-world datasets, focusing on performance of defense, recommendation, and efficiency. Additionally, we conduct an ablation study to comprehensively analyze the role of the proposed loss components.

**Table 1: Summary of datasets.**

Dataset	Attribute	Category #	User #	Item #	Rating #	Sparsity
ML-1M	Gender	2	6,040	3,416	999,611	95.155%
	Age	3				
LFM-2B	Gender	2	19,972	99,639	2,829,503	99.858%
	Age	3				
KuaiSAR	Feat1	7	21,852	140,367	2,166,893	99.929%
	Feat2	2				
Last.fm-360K	Gender	2	130,046	11,835	6,450,050	99.581%
	Age	3				

### 5.1 Experimental Settings

*Datasets.* The experiments are conducted on four real-world public datasets, each comprising user-item interaction data and user attribute data. The user attribute data includes sensitive information such as gender, age, and location. Detailed information about the datasets is as follows:

- **MovieLens 1M (ML-1M):** A version of MovieLens dataset that has 1 million ratings.
- **LFM-2B<sup>1</sup>:** This dataset collected more than 2 billion listening events, which are used for music retrieval and recommendation tasks [42]. Here, we use a subset of the whole dataset which includes more than 3 million ratings.
- **KuaiSAR<sup>2</sup>:** KuaiSAR is a unified search and recommendation dataset containing user behavior logs collected from the short-video mobile app, Kuaishou<sup>3</sup>. Here we use a tiny version of KuaiSAR, i.e., KuaiSAR-small.
- **Last.fm-360K<sup>4</sup>:** This dataset contains approximately 17 million listening events from nearly 360,000 users, and is commonly used for music retrieval and recommendation tasks [8].

The characteristics are summarized in Table 1.

*Recommendation models.* We validate the effectiveness of our method on three mainstream recommendation models. These models represent three common structural types mentioned in Section 2.1, including Matrix Factorization-based CF, Neural Network-based CF, and Graph-based CF.

- **DMF:** Deep Matrix Factorization [57] is one of the representative models based on matrix factorization.
- **NCF:** Neural Collaborative Filtering [27] is a classical CF model based on neural networks.
- **LightGCN:** Light Graph Convolution Network [26] is the State-Of-The-Art (SOTA) CF model that improves recommendation performance by simplifying graph convolution network.

*Evaluation Metrics.* We evaluate the performance of defense and recommendation using the following metrics.

- **Defense.** Aligning consistently with [39], attackers can train a robust adversarial classifier with machine learning models. To quantify the effectiveness of the defense, we utilize two commonly used classification metrics: the micro-averaged F1 score (F1) and Balanced Accuracy (BAcc) to assess the performance

<sup>1</sup><http://www.cp.jku.at/datasets/LFM-2b>

<sup>2</sup><https://kuaisar.github.io/>

<sup>3</sup><https://www.kuaishou.com/>

<sup>4</sup><http://ocelma.net/MusicRecommendationDataset/lastfm-360K.html>

of AIA [16, 22]. Lower values of F1 and BAcc indicate a more effective defense. According to existing literature [6, 58], we train the attacker using 80% of the users, with the remaining 20% used for testing. The outcomes of the AIA are obtained through five-fold cross-validation, averaged over five runs. To ensure a fair comparison, we optimized the hyperparameters until the loss function converged to obtain the optimal defensive effect.

- **Recommendation.** To assess the recommendation performance, we employ the leave-one-out testing [27]. We utilize Hit Rate at rank  $K$  (HR@ $K$ ) and Normalized Discounted Cumulative Gain at rank  $K$  (NDCG@ $K$ ) as recommendation metrics. HR@ $K$  measures whether the test item appears in the top- $K$  list, while NDCG@ $K$  is a position-aware ranking metric that assigns higher scores to hits at higher positions [25, 57]. In this paper, we calculate HR@ $K$  and NDCG@ $K$  using the entire set of negative items rather than a sampled subset, due to observed instability and inconsistency issues with sampled metrics compared to their precise versions [38]. Note that we compare the recommendation performance of various methods when achieving optimal defense effects separately.

*Compared baselines.* Although the setting of PoT differs from that of InT, comparing our proposed InT methods with PoT approaches contributes to a comprehensive understanding of the problem. Therefore, we compare our proposed methods with three representative baselines:

- **Original:** This is the original model without defense.
- **DP (DP-PoT):** This method protects user attributes by introducing noise perturbations to the original training data [62]. Under the gray-box setting in this paper, DP is implemented by adding noise to embedding layer parameters.
- **AU (AU-PoT):** This represents the current SOTA PoT method [39]. It optimizes a two-component loss.
- **Adv (Adv-InT):** This method uses adversarial training to achieve attribute defense for the MultVAE [16]. We also apply the idea of adversarial training to our tested recommendation models, i.e., DMF, NCF, and LightGCN.

*Hardware Information.* All models and algorithms are implemented with Python 3.8 and PyTorch 1.9. We run all experiments on an Ubuntu 20.04 System server with 256GB RAM and NVIDIA GeForce RTX 4090 GPU.

We run all models 10 times and report the average results. We provide details of dataset pre-processing and parameter settings in Appendix B.

## 5.2 Results

*Defense performance.* Protecting the target attributes is our primary focus. The performance of the defense is assessed by the performance of the attacker, i.e., an MLP. From the results in Table 2, we make the following observations. Firstly, the attacker achieves an average F1 score of 0.5322 and BAcc of 0.5320 on the original user embeddings, indicating that user attribute information embedded in user embeddings can be inferred by the attacker. Secondly, all methods can protect the attribute information contained in user embeddings to varying degrees. The methods of DP-PoT, AU-PoT, Adv-InT, and RAID reduce the F1 score by an average of

**Table 2: Performance of attribute inference attack. The top results are highlighted in bold.**

Dataset	Attribute	Method	DMF		NCF		LightGCN	
			F1	BAcc	F1	BAcc	F1	BAcc
ML-1M	Gender	Original	0.7501	0.7487	0.7545	0.7485	0.6987	0.7023
		DP-PoT	0.4425	<b>0.4425</b>	0.7318	0.7341	0.4290	<b>0.4290</b>
		AU-PoT	0.4868	0.4910	0.2889	0.5000	0.4047	0.5016
		Adv-InT	0.6180	0.6106	0.3042	0.5182	0.5626	0.5980
		RAID	<b>0.2666</b>	0.5000	<b>0.2665</b>	<b>0.4999</b>	<b>0.2667</b>	0.5000
	Age	Original	0.6221	0.6222	0.6241	0.6241	0.5664	0.5664
		DP-PoT	0.4254	0.4255	0.6109	0.6109	0.4155	0.4155
		AU-PoT	0.3336	<b>0.3333</b>	<b>0.3151</b>	0.4998	0.3333	<b>0.3333</b>
		Adv-InT	0.5994	0.5995	0.4524	0.4524	0.3923	0.3923
		RAID	<b>0.3334</b>	<b>0.3333</b>	0.3832	<b>0.3834</b>	<b>0.3331</b>	<b>0.3333</b>
LFM-2B	Gender	Original	0.6717	0.6802	0.6808	0.6779	0.6219	0.6162
		DP-PoT	0.5552	0.5559	0.6727	0.6691	0.3336	<b>0.3336</b>
		AU-PoT	0.5109	0.5088	0.4526	<b>0.4469</b>	0.4816	0.4701
		Adv-InT	0.6336	0.6259	0.6129	0.6163	0.5704	0.5733
		RAID	<b>0.3999</b>	<b>0.5000</b>	<b>0.2667</b>	0.5000	<b>0.3110</b>	0.5000
	Age	Original	0.3376	0.3378	0.3334	0.3341	0.3362	0.3362
		DP-PoT	<b>0.3333</b>	0.3338	0.3328	0.3324	0.3333	0.3332
		AU-PoT	<b>0.3333</b>	<b>0.3333</b>	<b>0.3160</b>	<b>0.3159</b>	0.3325	0.3323
		Adv-InT	0.3338	<b>0.3333</b>	0.3333	0.3333	0.3206	0.3207
		RAID	<b>0.3333</b>	<b>0.3333</b>	0.3317	0.3333	<b>0.3185</b>	<b>0.3193</b>
KuaiSAR	Feat1	Original	0.2530	0.2373	0.1522	0.1500	0.2160	0.2132
		DP-PoT	0.1603	0.1569	0.1549	0.1590	0.1042	0.1250
		AU-PoT	0.1275	0.1375	0.1203	0.1250	0.1249	0.1222
		Adv-InT	0.1182	0.1417	0.10665	0.1278	0.1531	0.1556
		RAID	<b>0.1042</b>	<b>0.1250</b>	<b>0.0949</b>	<b>0.1125</b>	<b>0.0972</b>	<b>0.1167</b>
	Feat2	Original	0.5685	0.5685	0.4242	0.4333	0.5564	0.5833
		DP-PoT	0.4394	0.4444	0.5503	0.5777	<b>0.2782</b>	<b>0.3333</b>
		AU-PoT	0.5490	0.5544	<b>0.1309</b>	<b>0.1311</b>	0.3558	0.3630
		Adv-InT	0.4006	0.4037	0.2848	0.3407	<b>0.2782</b>	<b>0.3333</b>
		RAID	<b>0.2782</b>	<b>0.3333</b>	0.2781	0.3333	<b>0.2782</b>	<b>0.3333</b>
Last.fm-360K	Gender	Original	0.7017	0.7119	0.7073	0.7159	0.7300	0.7310
		DP-PoT	0.6721	0.6825	0.6731	0.6782	0.6672	0.6691
		AU-PoT	0.7015	0.7055	0.6983	0.7005	0.7228	0.7246
		Adv-InT	0.4922	0.5052	0.9821	0.9822	0.7818	0.7787
		RAID	<b>0.4857</b>	<b>0.4862</b>	<b>0.3111</b>	<b>0.5000</b>	<b>0.6242</b>	<b>0.6438</b>
	Age	Original	0.5658	0.5658	0.5373	0.5373	0.5789	0.5789
		DP-PoT	0.4621	0.4657	0.5061	0.5061	0.5146	0.5146
		AU-PoT	0.5394	0.5394	0.4855	0.4855	0.5580	0.5580
		Adv-InT	<b>0.4077</b>	<b>0.4077</b>	0.6315	0.6315	0.5514	0.5514
		RAID	0.4356	0.4356	<b>0.3333</b>	<b>0.3333</b>	<b>0.4865</b>	<b>0.4762</b>

16.68%, 25.30%, 15.92%, and 41.35%, respectively. At the same time, AU-PoT, Adv-InT, and RAID can reduce the BAcc by an average of 21.57%, 12.96%, and 28.85%, respectively. In contrast, DP-PoT only reduces BAcc by 19.15%. For binary attributes such as gender and multi-class attributes such as age, the BAcc of attackers using the RAID method post-defense is equivalent to that of a random attacker. This indicates that our proposed RAID method can effectively protect private attributes in recommendation models, whether they are binary or multi-class.

*Recommendation performance.* Recommendation performance is another crucial objective we must consider, as the process of protecting user privacy attributes typically comes at the cost of sacrificing model accuracy. To verify the effectiveness of the RAID framework in maintaining recommendation performance, we employ NDCG and HR for evaluation, truncating the ranking lists at 5, 10, 15, and 20. As shown in Tables 3 and 12 (in Appendix B), protecting user attributes against does impact recommendation performance. It is also noticeable that methods based on the PoT setting exhibit a significant decline in recommendation performance compared to those based on the InT approach. Specifically, compared to the original performance, PoT methods such as DP-PoT and AU-PoT

**Table 3: Results of recommendation performance with truncating the ranking list for these metrics at 5 and 10. The top results are highlighted in bold.**

Dataset	Attribute	Method	DMF				NCF				LightGCN			
			HR@5	NDCG@5	HR@10	NDCG@10	HR@5	NDCG@5	HR@10	NDCG@10	HR@5	NDCG@5	HR@10	NDCG@10
ML-1M	Gender	Original	0.0630	0.0390	0.1040	0.0520	0.0660	0.0410	0.1060	0.0540	0.0600	0.0370	0.1000	0.0500
		DP-PoT	0.0290	0.0180	0.0490	0.0240	0.0090	0.0050	0.0150	0.0070	0.0260	0.0170	0.0420	0.0220
		AU-PoT	<b>0.0600</b>	<b>0.0380</b>	<b>0.1000</b>	<b>0.0510</b>	0.0480	0.0320	0.0800	0.0420	0.0500	0.0320	0.0800	0.0410
		Adv-InT	0.0560	0.0350	0.0970	0.0490	0.0530	0.0320	0.0980	0.0470	0.0510	0.0320	0.0830	0.0430
	RAID	0.0540	0.0340	0.0890	0.0460	<b>0.0530</b>	<b>0.0330</b>	<b>0.0980</b>	<b>0.0470</b>	<b>0.0550</b>	<b>0.0340</b>	<b>0.0850</b>	<b>0.0440</b>	
	Age	Original	0.0630	0.0390	0.1040	0.0520	0.0660	0.0410	0.1060	0.0540	0.0600	0.0370	0.1000	0.0500
		DP-PoT	0.0220	0.0130	0.0440	0.0200	0.0090	0.0050	0.0150	0.0070	0.0250	0.0160	0.0430	0.0210
		AU-PoT	0.0500	0.0330	0.0850	0.0430	0.0570	0.0370	0.0950	0.0490	0.0510	0.0320	0.0790	0.0410
Adv-InT		0.0510	0.0330	0.0880	0.0450	0.0550	0.0340	0.0990	0.0480	0.0450	0.0290	0.0740	0.0380	
RAID	<b>0.0540</b>	<b>0.0340</b>	<b>0.0880</b>	<b>0.0450</b>	<b>0.0590</b>	<b>0.0380</b>	<b>0.1010</b>	<b>0.0520</b>	<b>0.0550</b>	<b>0.0340</b>	<b>0.0890</b>	<b>0.0450</b>		
LFM-2B	Gender	Original	0.0120	0.0070	0.0200	0.0100	0.0170	0.0100	0.0280	0.0140	0.0220	0.0140	0.0340	0.0180
		DP-PoT	0.0030	0.0010	0.0050	0.0020	0.0010	0.0010	0.0020	0.0010	0.0040	0.0020	0.0060	0.0030
		AU-PoT	0.0050	0.0030	0.0080	0.0040	0.0110	0.0070	0.0200	0.0100	<b>0.0210</b>	<b>0.0130</b>	<b>0.0320</b>	<b>0.0170</b>
		Adv-InT	0.0080	0.0050	0.0160	0.0070	0.0120	0.0070	0.0210	0.0100	0.0190	0.0110	0.0300	0.0150
	RAID	<b>0.0090</b>	<b>0.0050</b>	<b>0.0180</b>	<b>0.0080</b>	<b>0.0140</b>	<b>0.0090</b>	<b>0.0240</b>	<b>0.0120</b>	0.0190	0.0120	0.0310	0.0160	
	Age	Original	0.0120	0.0070	0.0200	0.0100	0.0170	0.0100	0.0280	0.0140	0.0220	0.0140	0.0340	0.0180
		DP-PoT	0.0020	0.0010	0.0050	0.0020	0.0010	0.0010	0.0020	0.0010	0.0030	0.0020	0.0050	0.0030
		AU-PoT	0.0100	0.0060	0.0150	0.0080	0.0110	0.0070	0.0200	0.0100	0.0200	<b>0.0130</b>	<b>0.0320</b>	<b>0.0170</b>
Adv-InT		0.0080	0.0050	0.0160	0.0080	0.0130	0.0080	0.0220	0.0110	0.0160	0.0100	0.0280	0.0140	
RAID	<b>0.0110</b>	<b>0.0070</b>	<b>0.0170</b>	<b>0.0090</b>	<b>0.0170</b>	<b>0.0110</b>	<b>0.0260</b>	<b>0.0140</b>	<b>0.0200</b>	0.0120	0.0310	0.0150		
KuaiSAR	Feat1	Original	0.0190	0.0120	0.0310	0.0150	0.0180	0.0110	0.0320	0.0150	0.0200	0.0130	0.0360	0.0180
		DP-PoT	0.0040	0.0020	0.0080	0.0040	0.0020	0.0010	0.0050	0.0020	0.0060	0.0040	0.0110	0.0050
		AU-PoT	0.0150	0.0100	0.0270	0.0130	0.0180	0.0110	0.0300	0.0150	0.0190	0.0120	0.0320	0.0160
		Adv-InT	0.0190	0.0120	0.0310	0.0150	0.0150	0.0100	0.0260	0.0140	0.0120	0.0080	0.0210	0.0100
	RAID	<b>0.0190</b>	<b>0.0120</b>	<b>0.0320</b>	<b>0.0160</b>	<b>0.0160</b>	<b>0.0110</b>	<b>0.0300</b>	<b>0.0150</b>	<b>0.0190</b>	<b>0.0120</b>	<b>0.0330</b>	<b>0.0160</b>	
	Feat2	Original	0.0170	0.0100	0.0300	0.0150	0.0180	0.0110	0.0320	0.0150	0.0200	0.0130	0.0360	0.0180
		DP-PoT	0.0030	0.0020	0.0050	0.0020	0.0020	0.0010	0.0050	0.0020	0.0050	0.0030	0.0100	0.0050
		AU-PoT	0.0140	0.0090	0.0270	0.0130	0.0160	<b>0.0110</b>	<b>0.0300</b>	<b>0.0150</b>	0.0160	0.0100	0.0290	0.0140
Adv-InT		0.0090	0.0050	0.0190	0.0080	0.0080	0.0050	0.0160	0.0080	0.0110	0.0070	0.0180	0.0090	
RAID	<b>0.0160</b>	<b>0.0090</b>	<b>0.0290</b>	<b>0.0130</b>	<b>0.0170</b>	0.0100	0.0290	0.0140	<b>0.0190</b>	<b>0.0120</b>	<b>0.0320</b>	<b>0.0160</b>		
last.FM 360K	Gender	Original	0.0630	0.0400	0.1050	0.0530	0.0630	0.0400	0.1070	0.0540	0.0670	0.0420	0.1120	0.0570
		DP-PoT	0.0520	0.0320	0.0880	0.0440	0.0500	0.0310	0.0870	0.0430	0.0180	0.0110	0.0300	0.0150
		AU-PoT	<b>0.0630</b>	<b>0.0400</b>	<b>0.1050</b>	<b>0.0530</b>	<b>0.0630</b>	<b>0.0400</b>	<b>0.1070</b>	<b>0.0540</b>	<b>0.0670</b>	<b>0.0420</b>	<b>0.1120</b>	<b>0.0570</b>
		Adv-InT	0.0610	0.0380	0.1020	0.0510	0.0620	0.0390	0.1040	0.0520	0.0550	0.0360	0.0910	0.0470
	RAID	<b>0.0630</b>	<b>0.0400</b>	<b>0.1050</b>	<b>0.0530</b>	0.0620	<b>0.0400</b>	0.1040	0.0530	<b>0.0670</b>	<b>0.0420</b>	<b>0.1120</b>	<b>0.0570</b>	
	Age	Original	0.0630	0.0400	0.1050	0.0530	0.0630	0.0400	0.1070	0.0540	0.0670	0.0420	0.1120	0.0570
		DP-PoT	0.0520	0.0320	0.0880	0.0440	0.0500	0.0310	0.0870	0.0430	0.0180	0.0110	0.0300	0.0150
		AU-PoT	<b>0.0630</b>	<b>0.0400</b>	<b>0.1050</b>	<b>0.0530</b>	<b>0.0640</b>	<b>0.0400</b>	<b>0.1070</b>	<b>0.0540</b>	<b>0.0670</b>	<b>0.0420</b>	<b>0.1120</b>	<b>0.0570</b>
Adv-InT		0.0600	0.0370	0.1010	0.0500	0.0570	0.0350	0.0980	0.0490	0.0620	0.0400	0.1030	0.0530	
RAID	<b>0.0630</b>	<b>0.0400</b>	<b>0.1050</b>	<b>0.0530</b>	0.0620	0.0390	0.1060	0.0530	<b>0.0670</b>	<b>0.0420</b>	<b>0.1120</b>	<b>0.0570</b>		

show an average reduction in NDCG of 59.44% and 8.53% respectively, and a decrease in HR of 58.46% and 9.86% respectively. In contrast, the InT method, i.e., Adv-InT, show an average decrease of only 14.76% in NDCG and 14.73% in HR. RAID, which is also an InT method, records an average decline of 6.01% in NDCG and 6.44% in HR, achieving optimal performance across each dataset and model. Our proposed RAID surpasses Adv-InT in maintaining recommendation performance because our defense approach, which aligns distributions, does not interfere with other relevant information within user embeddings. This preservation of essential embedding features ensures that the recommendation capability remains robust despite the implementation of privacy-preserving measures.

*Ablation study.* Table 4 presents the results of an ablation study conducted using NCF on the ML-1M dataset. We sequentially remove defense loss  $\mathcal{L}_D$  and recommendation loss  $\mathcal{L}_P$  to assess their impact on the defense (F1 and BAcc) and recommendation (HR and

NDCG) performance. Initially, when we remove defense loss  $\mathcal{L}_D$ , we observe a significant increase in the attacker’s performance. This indicates that without active defense measures, attackers can easily extract private attribute information from user embeddings. Subsequently, when we remove recommendation loss  $\mathcal{L}_P$ , although the model performed well in defending against attackers, there is a noticeable decline in recommendation performance. This suggests that removing this component of the loss, while allowing the model to remain secure, significantly impairs its recommendation capabilities, decreasing its utility. These results from the ablation study clearly demonstrate the critical roles of defense loss  $\mathcal{L}_D$  and recommendation loss  $\mathcal{L}_P$  in our proposed RAID. The former primarily affects the effectiveness of defense, while the latter ensures the model’s utility.

**Table 4: Results of ablation studies.**

$\mathcal{L}_D$	$\mathcal{L}_P$	F1	BAcc	HR@10	NDCG@10
✓	✓	0.2665	0.4999	0.0980	0.0470
✗	✓	0.7545	0.7485	0.1060	0.0540
✓	✗	0.3973	0.5002	0.0600	0.0290

**Table 5: Impacts of PoT and InT settings.**

Settings	AU-PoT		Adv-InT		RAID	
	HR@10	NDCG@10	HR@10	NDCG@10	HR@10	NDCG@10
PoT	0.1530	0.0830	0.1491	0.0720	0.1500	0.0810
InT	0.1540	0.0835	0.1510	0.0740	0.1550	0.0850

## 6 DISCUSSIONS

In this section, we discuss the limitations present in existing methods and further validate the effectiveness of our proposed RAID. Furthermore, we examine the effectiveness of RAID in defending against attacks targeting multiple attributes and provide a detailed discussion of RAID’s limitations in Appendix C.

### 6.1 Limitation of Existing Methods

In response to the limitations of existing methods outlined in Section 1, we conduct individual verifications. These evaluations analyze the differences between PoT and InT in their ability to preserve recommendation performance and the effectiveness of defense.

*PoT vs InT.* To verify the differing impacts of PoT and InT settings on preserving recommendation performance, we attempt to extend them to another setting. We control the methods under these two settings to achieve similar defensive performance and compare their effects on preserving recommendation performance. Note that DP can only be operated under the PoT setting. We validate the performance of model NCF on dataset ML-100K (Gender), and the results are presented in Table 5. We have the following two observations: i) Except for DP, the recommendation performance under the InT setting significantly surpasses that under the PoT setting, confirming our hypothesis; and ii) Our proposed RAID shows superior recommendation performance in the InT setting compared to the existing methods, indicating that RAID is more compatible with InT.

*Effectiveness of the Defense.* Existing defense methods lack theoretical guarantees, making it uncertain whether they can effectively safeguard against attacks. Our method addresses this limitation. We define the defense objective as minimizing the distance between class distributions of protected attributes, thereby preventing attackers from training a classifier for effective separation. We validate this on datasets ML-100K, ML-1M, LFM-2B, KuaiSAR, and model NCF by comparing the class distributions of user embeddings in the original model with those after protection, as illustrated in Figure 4. We compress the user embeddings to one dimension using PCA, retaining the direction with the maximum variance in the data. We present the histogram of class distributions in Figure 4, with each color representing a different class. As shown in the first row

**Table 6: Performance of attribute inference attack w.r.t. different types of non-DNN-based attacker. The top results are highlighted in bold.**

Attribute	Method	DT		SVM		NB		KNN	
		F1	BAcc	F1	BAcc	F1	BAcc	F1	BAcc
Gender	Original	0.6391	0.6379	0.7500	0.7496	0.7271	0.7306	0.7018	0.6981
	DP-PoT	0.5378	0.5437	0.6459	0.6358	0.6451	0.6428	0.5617	0.5679
	AU-PoT	<b>0.5043</b>	<b>0.5152</b>	0.4503	0.4637	<b>0.4737</b>	0.4696	0.5042	0.5006
	Adv-InT	0.5224	0.5234	0.6193	0.6264	0.5303	0.5290	0.5870	0.5977
	RAID	0.5151	0.5197	<b>0.3995</b>	<b>0.4096</b>	0.4762	<b>0.4556</b>	<b>0.4042</b>	<b>0.4292</b>
Age	Original	0.4646	0.4646	0.6130	0.6130	0.5535	0.5535	0.5094	0.5093
	DP-PoT	0.3733	0.3733	0.4591	0.4591	0.4675	0.4674	0.4018	0.4018
	AU-PoT	0.3533	0.3533	0.2587	0.2587	0.2990	0.2989	0.2923	0.2923
	Adv-InT	0.5388	0.5388	0.5428	0.5428	0.5412	0.5412	0.6943	0.6943
	RAID	<b>0.3284</b>	<b>0.3284</b>	<b>0.2277</b>	<b>0.2277</b>	<b>0.2923</b>	<b>0.2923</b>	<b>0.2721</b>	<b>0.2721</b>

of Figure 4, there is a noticeable difference between the two class distributions for the original user embedding. This difference enables the attacker to easily distinguish between the classes, thereby inferring their corresponding attributes. In contrast, as shown in the second row of Figure 4, the RAID converges different class distributions towards a single centroid distribution, thereby validating the effectiveness of our defense strategy.

### 6.2 Robustness to Adaptive Attack

In real-life scenarios, numerous models are available for conducting AIA, often rendering the attacker unknown to the defender. To better validate the robustness of our method, we also investigate other types of attackers. Additionally, we adjust the amount of user data accessible to the attacker. Specifically, we use gender and age as target attributes and conduct validations on the ML-1M dataset.

*Non-DNN-based Attackers.* We explore several machine learning models commonly used in classification tasks as attackers, including Decision Tree (DT), Support Vector Machine (SVM), Naive Bayes (NB), and  $k$ -Nearest Neighbors (KNN). We observe from Table 6 that

- It is evident that our proposed RAID significantly outperforms other baselines, indicating that our method can more effectively protect attribute information from the recommendation model and safeguard user privacy when facing unknown attacker models. Specifically, DP-PoT, AU-PoT, Adv-InT, and RAID respectively reduced the BAcc by 17.45%, 36.40%, 7.31%, and 40.79%. In most cases, the BAcc after RAID defense was similar to that of a random attacker.
- The defense effectiveness of Adv-InT, which is trained against specific DNN-based inference models, deteriorates when faced with non-DNN-based models. Specifically, when the attacker is an MLP, Adv-InT reduced the BAcc by 9.25%, but when the attacker was not an MLP, the average reduction was only 7.31%.
- DNN-based attackers (i.e., MLP) generally perform better than other attackers in most scenarios due to their ability to learn non-linear associations between user embeddings and target attribute labels.

*Ensemble Learning-based Attackers.* Ensemble learning is a widely used technique to enhance the performance of classification models. We explore several well-recognized ensemble learning-based attackers, including Random Forest (RF), AdaBoost, XGBoost, and

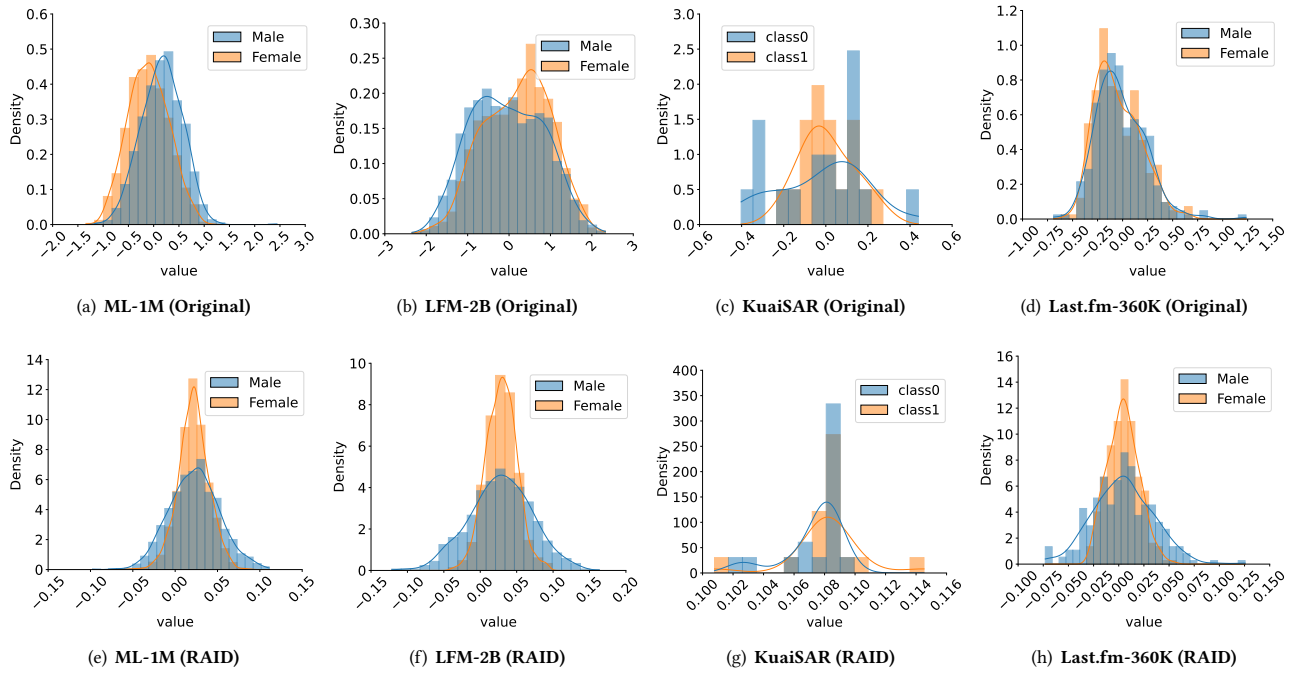


Figure 4: Distribution of user embedding on NCF, where different colors denote different class values (e.g., male vs. female).

Table 7: Performance of attribute inference attack w.r.t. different types of ensemble learning-based attackers. The top results are highlighted in bold.

Attribute	Method	RF		AdaBoost		XGBoost		GBDT	
		F1	BAcc	F1	BAcc	F1	BAcc	F1	BAcc
Gender	Original	0.6927	0.6947	0.7373	0.7381	0.7101	0.7124	0.7097	0.7100
	DP-PoT	0.5882	0.5919	0.6321	0.6319	0.6121	0.6115	0.6061	0.6077
	AU-PoT	0.5116	0.5049	<b>0.5100</b>	<b>0.5009</b>	0.5372	0.5497	0.5314	0.5375
	Adv-InT	0.5214	0.5253	0.5432	0.5319	0.5623	0.5708	0.5555	0.5614
	RAID	<b>0.4744</b>	<b>0.4947</b>	0.5194	0.5166	<b>0.5319</b>	<b>0.5348</b>	<b>0.5265</b>	<b>0.5299</b>
Age	Original	0.5111	0.5112	0.5898	0.5898	0.5951	0.5951	0.5863	0.5863
	DP-PoT	0.3983	0.3984	0.4423	0.4423	0.4325	0.4325	0.4201	0.4201
	AU-PoT	0.3481	0.3482	0.4423	0.4423	0.4325	0.4325	0.4201	0.4201
	Adv-InT	0.4509	0.4509	0.4825	0.4825	0.5527	0.5527	0.5558	0.5558
	RAID	<b>0.3236</b>	<b>0.3236</b>	<b>0.3316</b>	<b>0.3317</b>	<b>0.3440</b>	<b>0.2429</b>	<b>0.3332</b>	<b>0.3333</b>

Gradient Boosting Decision Tree (GBDT). As shown from Table 7, i) Our proposed RAID framework consistently outperforms the compared baselines in terms of defensive performance against various ensemble learning-based attackers. This highlights the robustness of our RAID framework in safeguarding user privacy across different sophisticated attacking methods; and ii) Comparing the performance of various attackers on the original embedding, the MLP attacker still outperforms those based on ensemble learning. This indicates that while ensemble methods are effective, the MLP’s ability to capture complex patterns in data makes it a more formidable adversary in scenarios involving GIA.

*Different layers of MLP.* In previous experiments, we employed a two-layer MLP as the attacker and found that the MLP’s attack effectiveness was substantially stronger than other attack models.

Table 8: Performance of attribute inference attack w.r.t. different types of MLP-based attacker. The top results are highlighted in bold. The dimensions of layers are  $\{d_{out}\}$ ,  $\{100, d_{out}\}$ ,  $\{100, 64, d_{out}\}$ ,  $\{100, 64, 32, d_{out}\}$ , where  $d_{out}$  denotes the count of attribute categories.

Attribute	Method	Layer=1		Layer=2		Layer=3		Layer=4	
		F1	BAcc	F1	BAcc	F1	BAcc	F1	BAcc
Gender	Original	0.7481	0.7494	0.7530	0.7541	0.7408	0.7452	0.7451	0.7377
	DP-PoT	0.6469	0.6499	0.6425	0.6419	0.6459	0.6433	0.6090	0.6226
	AU-PoT	0.4683	0.4436	0.5177	0.4980	0.5339	0.5153	<b>0.3009</b>	<b>0.4962</b>
	Adv-InT	0.5258	0.5169	0.6155	0.6101	0.6345	0.6422	0.6349	0.6338
	RAID	<b>0.4588</b>	0.4549	<b>0.4832</b>	<b>0.4709</b>	<b>0.3110</b>	<b>0.5000</b>	0.4000	0.5000
Age	Original	0.6191	0.6191	0.6226	0.6226	0.6147	0.6147	0.6120	0.6120
	DP-PoT	0.4261	0.4261	0.4491	0.4490	0.4419	0.4420	0.4251	0.4251
	AU-PoT	0.3267	0.3267	0.3334	0.3333	0.3331	0.3331	0.3329	0.3329
	Adv-InT	0.5519	0.5519	0.7116	0.7116	0.6558	0.6557	0.6283	0.6283
	RAID	<b>0.2990</b>	<b>0.2990</b>	<b>0.3314</b>	<b>0.3341</b>	<b>0.3211</b>	<b>0.3212</b>	<b>0.3298</b>	<b>0.3240</b>

To further explore the robustness of our method, in this experiment, we investigate the impact of different MLP architectures. Specifically, we examine the effects of varying the number of layers: 1, 2, 3, and 4. From the results presented in Table 8, we observe that the two-layer MLP performs the best among all the compared attackers. Additionally, increasing the number of layers does not enhance attack performance. We also note that our proposed RAID outperforms other comparative methods in most cases, confirming the effectiveness of RAID in defending against increasingly complex MLP architectures. This suggests that our defense mechanism is not only effective against sophisticated attacks but also adaptable to variations in attack model complexities.

*Different ratio of leaked data.* In real-world scenarios, the amount of data accessible to attackers is often unclear. Based on this consideration, we adjust the proportion of user data that the attacker could obtain, specifically setting it to 20%, 40%, 60%, and 80% for testing on an MLP. The experimental results, as shown in Table 10, indicate the following observations: i) Once the attacker possesses 40% of the data, they already have the capability to effectively infer user privacy attributes; and ii) Our method is minimally affected by variations in the percentage of data available to the attacker, showing insensitivity to these changes and consistently achieving effective defensive outcomes. This resilience highlights the robustness of our approach to safeguarding user privacy against varying levels of data exposure to attackers.

### 6.3 Parameter Sensitivity Analysis

We conduct an in-depth analysis of the performance fluctuations of our method under different hyper-parameter settings, i.e., the penalization coefficient  $\eta$  and the frequency  $\xi$  of centroid distribution computation. Specifically, we adjust the values of  $\eta$  and  $\xi$  while keeping other hyper-parameters constant.

*Penalization coefficient  $\eta$ .* Regarding the penalization coefficient  $\eta$ , as depicted in Figure 5, we set  $\eta$  values to 0.4, 0.8, 1.2, 1.6, 2.0, and 2.4. To measure defensive and recommendation performance, we used BAcc and NDCG@10 as evaluation metrics. We observe that our proposed RAID exhibits good robustness in terms of NDCG@10 across different  $\eta$  values. Simultaneously, we find that increasing  $\eta$  leads to a decrease in BAcc. This observation suggests that RAID can enhance defensive effectiveness with only a slight sacrifice in recommendation performance. Additionally, in multi-class scenarios (Figure 5(c), 7 classes for Feat1), RAID incurs less performance loss while enhancing defense effectiveness, which might be due to the centroid distribution calculated in multi-class scenarios retaining more information other than the protected attribute compared to the original class-conditional distribution.

*Frequency  $\xi$ .* Concerning the frequency  $\xi$  of centroid distribution computation, we compare model performance with  $\xi$  values of 1, 2, 3, and 4. The experimental results, as shown in Table 9, demonstrate that our proposed RAID's defensive (i.e., F1 and BAcc) and recommendation (i.e., HR@10 and NDCG@10) performance also exhibit good robustness to different  $\xi$  values. Although changes were not substantial, the BAcc metric slightly decreased as  $\xi$  was reduced. Meanwhile, as  $\xi$  increased, the training convergence time of the model noticeably decreased.

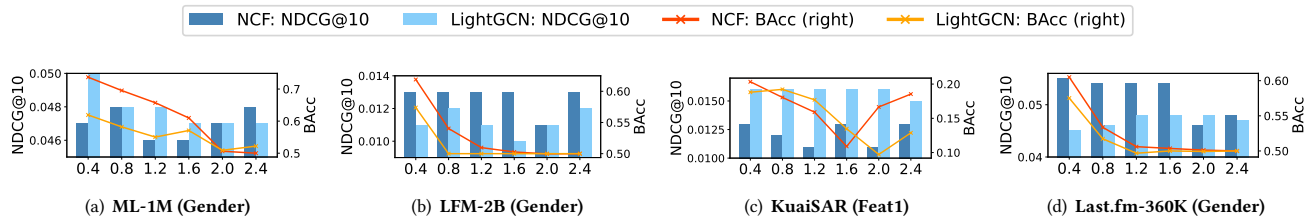
## 7 CONCLUSION

In this work, we propose a practical two-stage framework named RAID for defending against AIA in recommender systems. Specifically, RAID aligns the attribute distributions to an ideal centroid distribution with constraints to make attributes indistinguishable, thereby defending against AIA while preserving recommendation performance. In phase I, RAID is trained directly on the training data to achieve initial recommendation performance. In phase II, RAID first obtains the ideal centroid distribution by solving a constrained Wasserstein-2 centroid optimization problem based on the distribution of each class in the protected attribute. Subsequently, during

the training process, RAID employs optimal transport to align the distribution of each class toward this centroid distribution, thereby defending against AIA. Our empirical results on real-world datasets and mainstream recommendation models demonstrate that: i) Our proposed method significantly outperforms existing baselines in terms of defense effectiveness; ii) Our proposed method has minimal impact on the recommendation performance of the model; iii) Our proposed method shows significant efficiency improvements and easier convergence compared to adversarial training methods; and iv) Our proposed method is applicable to both binary and multi-class attributes. Notably, RAID is effective against gray-box attacks and can be extended to address fairness issues in recommender systems.

## REFERENCES

- [1] Gediminas Adomavicius and Alexander Tuzhilin. 2010. Context-aware recommender systems. In *Recommender systems handbook*. Springer, 217–253.
- [2] Martial Agueh and Guillaume Carlier. 2011. Barycenters in the Wasserstein space. *SIAM Journal on Mathematical Analysis* 43, 2 (2011), 904–924.
- [3] Martin Arjovsky, Soumith Chintala, and Léon Bottou. 2017. Wasserstein generative adversarial networks. In *International conference on machine learning*. PMLR, 214–223.
- [4] Raghavendran Balu and Teddy Furon. 2016. Differentially private matrix factorization using sketching techniques. In *Proceedings of the 4th ACM Workshop on Information Hiding and Multimedia Security*. 57–62.
- [5] Ghazaleh Beigi and Huan Liu. 2018. Similar but different: Exploiting users' congruity for recommendation systems. In *Social, Cultural, and Behavioral Modeling: 11th International Conference, SBP-BRIMS 2018, Washington, DC, USA, July 10-13, 2018, Proceedings 11*. Springer, 129–140.
- [6] Ghazaleh Beigi, Ahmadreza Mosallanezhad, Ruocheng Guo, Hamidreza Alvari, Alexander Nou, and Huan Liu. 2020. Privacy-aware recommendation with private-attribute protection using adversarial learning. In *Proceedings of the 13th International Conference on Web Search and Data Mining*. 34–42.
- [7] Jean-David Benamou, Guillaume Carlier, Marco Cuturi, Luca Nenna, and Gabriel Peyré. 2015. Iterative Bregman projections for regularized transportation problems. *SIAM Journal on Scientific Computing* 37, 2 (2015), A1111–A1138.
- [8] O. Celma. 2010. *Music Recommendation and Discovery in the Long Tail*. Springer.
- [9] Abdelberri Chaabane, Gergely Acs, Mohamed Ali Kaafar, et al. 2012. You are what you like! information leakage through users' interests. In *Proceedings of the 19th annual network & distributed system security symposium (NDSS)*. Citeseer.
- [10] Marco Cuturi. 2013. Sinkhorn distances: Lightspeed computation of optimal transport. *Advances in neural information processing systems* 26 (2013).
- [11] Marco Cuturi and Arnaud Doucet. 2014. Fast computation of Wasserstein barycenters. In *International conference on machine learning*. PMLR, 685–693.
- [12] Ishan Deshpande, Ziyu Zhang, and Alexander G Schwing. 2018. Generative modeling using the sliced Wasserstein distance. In *Proceedings of the IEEE conference on computer vision and pattern recognition*. 3483–3491.
- [13] Gustavo Escobedo, Christian Ganhör, Stefan Brandl, Mirjam Augstein, and Markus Schedl. 2024. Simultaneous Unlearning of Multiple Protected User Attributes From Variational Autoencoder Recommenders Using Adversarial Training. In *Advances in Bias and Fairness in Information Retrieval - 5th International Workshop, BIAS 2024, Washington, DC, USA, July 18, 2024, Revised Selected Papers*, Vol. abs/2410.20965. 91–102.
- [14] Matt Fredrikson, Somesh Jha, and Thomas Ristenpart. 2015. Model inversion attacks that exploit confidence information and basic countermeasures. In *Proceedings of the 22nd ACM SIGSAC conference on computer and communications security*. 1322–1333.
- [15] Matthew Fredrikson, Eric Lantz, Somesh Jha, Simon Lin, David Page, and Thomas Ristenpart. 2014. Privacy in pharmacogenetics: An {End-to-End} case study of personalized warfarin dosing. In *23rd USENIX security symposium (USENIX Security 14)*. 17–32.
- [16] Christian Ganhör, David Penz, Navid Rekasaz, Oleg Lesota, and Markus Schedl. 2022. Unlearning protected user attributes in recommendations with adversarial training. In *Proceedings of the 45th International ACM SIGIR Conference on Research and Development in Information Retrieval*. 2142–2147.
- [17] Aude Genevay, Marco Cuturi, Gabriel Peyré, and Francis Bach. 2016. Stochastic optimization for large-scale optimal transport. *Advances in neural information processing systems* 29 (2016).
- [18] Clark R Givens and Rae Michael Shortt. 1984. A class of Wasserstein metrics for probability distributions. *Michigan Mathematical Journal* 31, 2 (1984), 231–240.
- [19] Oana Goga, Howard Lei, Sree Hari Krishnan Parthasarathi, Gerald Friedland, Robin Sommer, and Renata Teixeira. 2013. Exploiting innocuous activity for

Figure 5: Effect of the hyper-parameter penalization coefficient  $\eta$ .Table 9: Effect of the hyper-parameter frequency  $\xi$ .

Dataset	Model	1				2				3				4			
		F1	BAcc	HR@10	NDCG@10												
ML-1M	DMF	0.3110	0.4984	0.0980	0.0420	0.3598	0.5055	0.0830	0.0430	0.3135	0.4972	0.0840	0.0430	0.3454	0.5081	0.0870	0.0420
	NCF	0.3027	0.5045	0.0980	0.0480	0.4444	0.5000	0.0960	0.0490	0.3558	0.5005	0.0960	0.0480	0.2666	0.5000	0.0970	0.0480
	LightGCN	0.5340	0.5815	0.0960	0.0480	0.6401	0.6029	0.0960	0.0470	0.6527	0.5979	0.0940	0.0470	0.4593	0.5827	0.0920	0.0460
LFM-2B	DMF	0.4056	0.5110	0.0170	0.0090	0.2925	0.5005	0.0180	0.0080	0.3884	0.5067	0.0170	0.0080	0.3807	0.5109	0.0160	0.0070
	NCF	0.2121	0.5037	0.0260	0.0130	0.3554	0.5000	0.0240	0.0110	0.3555	0.5000	0.0240	0.0120	0.2769	0.5101	0.0240	0.0110
	LightGCN	0.3110	0.5000	0.0240	0.0110	0.3109	0.5000	0.0240	0.0110	0.3973	0.4972	0.0230	0.0110	0.3352	0.5017	0.0230	0.0110
KuaiSAR	DMF	0.2175	0.2409	0.0320	0.0160	0.2161	0.2361	0.0310	0.0150	0.1800	0.1958	0.0300	0.0160	0.2543	0.2708	0.0300	0.0150
	NCF	0.1736	0.1861	0.0250	0.0120	0.0972	0.1166	0.0290	0.0140	0.1205	0.1409	0.0250	0.0120	0.1183	0.1333	0.0290	0.0140
	LightGCN	0.1018	0.1222	0.0330	0.0160	0.1130	0.1361	0.0330	0.0150	0.1041	0.1250	0.0350	0.0170	0.1018	0.1222	0.0330	0.0160
Last.fm-360K	DMF	0.4918	0.5074	0.0880	0.0490	0.2612	0.5103	0.0730	0.0340	0.2663	0.5000	0.0730	0.0410	0.4672	0.5054	0.0690	0.0430
	NCF	0.1775	0.5152	0.0900	0.0570	0.2222	0.5000	0.0810	0.0520	0.1772	0.5000	0.0950	0.0610	0.4444	0.5000	0.0750	0.0500
	LightGCN	0.3994	0.5000	0.0810	0.0480	0.3563	0.5000	0.0810	0.0460	0.2216	0.5000	0.0810	0.0470	0.3105	0.5005	0.0800	0.0450

Table 10: Performance of attribute inference attack w.r.t. different leak ratio. The top results are highlighted in bold.

Attribute	Method	20%		40%		60%		80%	
		F1	BAcc	F1	BAcc	F1	BAcc	F1	BAcc
Gender	Original	0.6822	0.7092	0.7243	0.7296	0.7545	0.7524	0.7629	0.7568
	DP-PoT	0.7439	0.7433	0.7530	0.7390	0.7428	0.7470	0.7450	0.7496
	AU-PoT	0.4663	<b>0.4650</b>	0.5217	<b>0.5014</b>	0.5331	<b>0.5108</b>	0.5386	0.5336
	Adv-InT	0.5822	0.5887	0.5971	0.5962	0.6188	0.6037	0.6404	0.6238
	RAID	<b>0.2755</b>	0.5000	<b>0.3563</b>	0.5146	<b>0.4300</b>	0.5250	<b>0.4740</b>	<b>0.5325</b>
	LightGCN	0.3110	0.5000	0.0240	0.0110	0.3109	0.5000	0.0240	0.0110
Age	Original	0.5613	0.5611	0.5891	0.5881	0.6074	0.6045	0.6457	0.6341
	DP-PoT	0.5869	0.5898	0.5947	0.5945	0.6207	0.6200	0.6285	0.6289
	AU-PoT	<b>0.2983</b>	<b>0.2984</b>	<b>0.3032</b>	<b>0.3027</b>	<b>0.3178</b>	<b>0.3177</b>	<b>0.3184</b>	<b>0.3180</b>
	Adv-InT	0.4349	0.4191	0.4632	0.4583	0.4963	0.4955	0.5094	0.5095
	RAID	0.3342	0.3333	0.3321	0.3330	0.3457	0.3451	0.3532	0.3517
	LightGCN	0.3110	0.5000	0.0240	0.0110	0.3109	0.5000	0.0240	0.0110

correlating users across sites. In *Proceedings of the 22nd international conference on World Wide Web*. 447–458.

- [20] Neil Zhenqiang Gong and Bin Liu. 2016. You are who you know and how you behave: Attribute inference attacks via users' social friends and behaviors. In *25th USENIX Security Symposium (USENIX Security 16)*. 979–995.
- [21] Neil Zhenqiang Gong and Bin Liu. 2018. Attribute inference attacks in online social networks. *ACM Transactions on Privacy and Security (TOPS)* 21, 1 (2018), 1–30.
- [22] Margherita Grandini, Enrico Bagli, and Giorgio Visani. 2020. Metrics for multi-class classification: an overview. *arXiv preprint arXiv:2008.05756* (2020).
- [23] Tao Guo, Song Guo, Jiewei Zhang, Wenchao Xu, and Junxiao Wang. 2022. Efficient attribute unlearning: Towards selective removal of input attributes from feature representations. *arXiv preprint arXiv:2202.13295* (2022).
- [24] Zhongxuan Han, Chaochao Chen, Xiaolin Zheng, Meng Li, Weiming Liu, Binhui Yao, Yuyuan Li, and Jianwei Yin. 2024. Intra- and Inter-group Optimal Transport for User-Oriented Fairness in Recommender Systems. In *Thirty-Eighth AAAI Conference on Artificial Intelligence, AAAI, February 20-27, 2024, Vancouver, Canada*. 8463–8471.
- [25] Xiangnan He, Tao Chen, Min-Yen Kan, and Xiao Chen. 2015. Trirank: Review-aware explainable recommendation by modeling aspects. In *Proceedings of the 24th ACM international conference on information and knowledge management*. 1661–1670.

- [26] Xiangnan He, Kuan Deng, Xiang Wang, Yan Li, Yongdong Zhang, and Meng Wang. 2020. Lightgcn: Simplifying and powering graph convolution network for recommendation. In *Proceedings of the 43rd International ACM SIGIR conference on research and development in Information Retrieval*. 639–648.
- [27] Xiangnan He, Lizi Liao, Hanwang Zhang, Liqiang Nie, Xia Hu, and Tat-Seng Chua. 2017. Neural collaborative filtering. In *Proceedings of the 26th international conference on world wide web*. 173–182.
- [28] Bargav Jayaraman and David Evans. 2022. Are attribute inference attacks just imputation?. In *Proceedings of the 2022 ACM SIGSAC Conference on Computer and Communications Security*. 1569–1582.
- [29] Jinyuan Jia and Neil Zhenqiang Gong. 2018. {AttriGuard}: A practical defense against attribute inference attacks via adversarial machine learning. In *27th USENIX Security Symposium (USENIX Security 18)*. 513–529.
- [30] Ray Jiang, Aldo Pacchiano, Tom Stepleton, Heinrich Jiang, and Silvia Chiappa. 2020. Wasserstein fair classification. In *Uncertainty in artificial intelligence*. PMLR, 862–872.
- [31] L Kantorovich. 1942. On the transfer of masses (in Russian). In *Doklady Akademii Nauk*, Vol. 37. 227.
- [32] Achim Klenke. 2013. *Probability theory: a comprehensive course*. Springer Science & Business Media.
- [33] Daniel Kluver, Michael D Ekstrand, and Joseph A Konstan. 2018. Rating-based collaborative filtering: algorithms and evaluation. *Social information access: Systems and technologies* (2018), 344–390.
- [34] Joseph A Konstan and John Riedl. 2012. Recommender systems: from algorithms to user experience. *User modeling and user-adapted interaction* 22 (2012), 101–123.
- [35] Yehuda Koren. 2009. Collaborative filtering with temporal dynamics. In *Proceedings of the 15th ACM SIGKDD international conference on Knowledge discovery and data mining*. 447–456.
- [36] Alexander Korotin, Lingxiao Li, Justin Solomon, and Evgeny Burnaev. 2021. Continuous wasserstein-2 barycenter estimation without minimax optimization. *arXiv preprint arXiv:2102.01752* (2021).
- [37] Michal Kosinski, David Stillwell, and Thore Graepel. 2013. Private traits and attributes are predictable from digital records of human behavior. *Proceedings of the national academy of sciences* 110, 15 (2013), 5802–5805.
- [38] Walid Krichene and Steffen Rendle. 2020. On sampled metrics for item recommendation. In *Proceedings of the 26th ACM SIGKDD international conference on knowledge discovery & data mining*. 1748–1757.
- [39] Yuyuan Li, Chaochao Chen, Xiaolin Zheng, Yizhao Zhang, Zhongxuan Han, Dan Meng, and Jun Wang. 2023. Making users indistinguishable: Attribute-wise unlearning in recommender systems. In *Proceedings of the 31st ACM International Conference on Multimedia*. 984–994.

- [40] Frank McSherry and Ilya Mironov. 2009. Differentially private recommender systems: Building privacy into the netflix prize contenders. In *Proceedings of the 15th ACM SIGKDD international conference on Knowledge discovery and data mining*. 627–636.
- [41] Shaguftha Mehnaz, Sayanton V Dibbo, Roberta De Viti, Ehsanul Kabir, Björn B Brandenburg, Stefan Mangard, Ninghui Li, Elisa Bertino, Michael Backes, Emiliano De Cristofaro, et al. 2022. Are your sensitive attributes private? novel model inversion attribute inference attacks on classification models. In *31st USENIX Security Symposium (USENIX Security 22)*. 4579–4596.
- [42] Alessandro B Melchiorre, Navid Rekasaz, Emilia Parada-Cabaleiro, Stefan Brandl, Oleg Lesota, and Markus Schedl. 2021. Investigating gender fairness of recommendation algorithms in the music domain. *Information Processing & Management* 58, 5 (2021), 102666.
- [43] Yan Michalevsky, Aaron Schulman, Gunaa Arumugam Veerapandian, Dan Boneh, and Gabi Nakibly. 2015. {PowerSpy}: Location Tracking Using Mobile Device Power Analysis. In *24th USENIX Security Symposium (USENIX Security 15)*. 785–800.
- [44] Paul Milgrom and Ilya Segal. 2002. Envelope theorems for arbitrary choice sets. *Econometrica* 70, 2 (2002), 583–601.
- [45] Andriy Mnih and Russ R Salakhutdinov. 2007. Probabilistic matrix factorization. *Advances in neural information processing systems* 20 (2007).
- [46] Gaspard Monge. 1781. Mémoire sur la théorie des déblais et des remblais. *Mem. Math. Phys. Acad. Royale Sci.* (1781), 666–704.
- [47] Saemi Moon, Seunghyuk Cho, and Dongwoo Kim. 2023. Feature unlearning for generative models via implicit feedback. *arXiv preprint arXiv:2303.05699*, 2, 3 (2023).
- [48] Sashank Narain, Triet D Vo-Huu, Kenneth Block, and Guevara Noubir. 2016. Inferring user routes and locations using zero-permission mobile sensors. In *2016 IEEE Symposium on Security and Privacy (SP)*. IEEE, 397–413.
- [49] Janna Otterbacher. 2010. Inferring gender of movie reviewers: exploiting writing style, content and metadata. In *Proceedings of the 19th ACM international conference on Information and knowledge management*. 369–378.
- [50] Al Mamunur Rashid, Istvan Albert, Dan Cosley, Shyong K Lam, Sean M McNee, Joseph A Konstan, and John Riedl. 2002. Getting to know you: learning new user preferences in recommender systems. In *Proceedings of the 7th international conference on Intelligent user interfaces*. 127–134.
- [51] Yue Shi, Martha Larson, and Alan Hanjalic. 2014. Collaborative filtering beyond the user-item matrix: A survey of the state of the art and future challenges. *ACM Computing Surveys (CSUR)* 47, 1 (2014), 1–45.
- [52] Kai Shu, Suhang Wang, Jiliang Tang, Reza Zafarani, and Huan Liu. 2017. User identity linkage across online social networks: A review. *Acm Sigkdd Explorations Newsletter* 18, 2 (2017), 5–17.
- [53] Chiappa Silvia, Jiang Ray, Stepleton Tom, Pacchiano Aldo, Jiang Heinrich, and Aslanides John. 2020. A general approach to fairness with optimal transport. In *Proceedings of the AAAI Conference on Artificial Intelligence*, Vol. 34. 3633–3640.
- [54] Qinyong Wang, Hongzhi Yin, Tong Chen, Zi Huang, Hao Wang, Yanchang Zhao, and Nguyen Quoc Viet Hung. 2020. Next point-of-interest recommendation on resource-constrained mobile devices. In *Proceedings of the Web conference 2020*. 906–916.
- [55] Udi Weinsberg, Smriti Bhagat, Stratis Ioannidis, and Nina Taft. 2012. BlurMe: Inferring and obfuscating user gender based on ratings. In *Proceedings of the sixth ACM conference on Recommender systems*. 195–202.
- [56] Le Wu, Yonghui Yang, Kun Zhang, Richang Hong, Yanjie Fu, and Meng Wang. 2020. Joint item recommendation and attribute inference: An adaptive graph convolutional network approach. In *Proceedings of the 43rd International ACM SIGIR conference on research and development in Information Retrieval*. 679–688.
- [57] Hong-Jian Xue, Xinyu Dai, Jianbing Zhang, Shujian Huang, and Jiajun Chen. 2017. Deep matrix factorization models for recommender systems.. In *IJCAI*, Vol. 17. Melbourne, Australia, 3203–3209.
- [58] Shijie Zhang, Hongzhi Yin, Tong Chen, Zi Huang, Lizhen Cui, and Xiangliang Zhang. 2021. Graph embedding for recommendation against attribute inference attacks. In *Proceedings of the Web Conference 2021*. 3002–3014.
- [59] Shijie Zhang, Hongzhi Yin, Tong Chen, Quoc Viet Nguyen Hung, Zi Huang, and Lizhen Cui. 2020. Gcn-based user representation learning for unifying robust recommendation and fraudster detection. In *Proceedings of the 43rd international ACM SIGIR conference on research and development in information retrieval*. 689–698.
- [60] Yinqian Zhang, Ari Juels, Michael K Reiter, and Thomas Ristenpart. 2012. Cross-VM side channels and their use to extract private keys. In *Proceedings of the 2012 ACM conference on Computer and communications security*. 305–316.
- [61] Elena Zheleva and Lise Getoor. 2009. To join or not to join: the illusion of privacy in social networks with mixed public and private user profiles. In *Proceedings of the 18th international conference on World wide web*. 531–540.
- [62] Xue Zhu and Yuqing Sun. 2016. Differential privacy for collaborative filtering recommender algorithm. In *Proceedings of the 2016 ACM on international workshop on security and privacy analytics*. 9–16.

## A PROOFS AND OPTIMIZATION METHOD

### A.1 Proof of Lemma 1

We first present some prior results about the optimal transport problem.

With probability measures  $\mu, \nu$  on  $\mathcal{X}$ , we consider the the Wasserstein distance  $\mathcal{W}_2^2(\mu, \nu)$ , which is defined by

$$\mathcal{W}_2^2(\mu, \nu) := \min_{\pi \in \Pi(\mu, \nu)} \int_{\mathcal{X}^2} \|x - y\|_2^2 d\pi(x, y), \quad (14)$$

where  $\Pi(\mu, \nu)$  is the set of transport plans with marginals  $\mu$  and  $\nu$  on  $\mathcal{X}^2$ . Note that this expression is equivalent to Eq. (2) with the substitution of  $c(x, y)$  by  $\|x - y\|_2^2$ . Previous work [17] shows that dual and semi-dual formulation of wasserstein distance Eq. (14) are defined by

$$\begin{aligned} \mathcal{W}_2^2(\mu, \nu) &= \max_{\substack{f, g \in C(\mathcal{X}) \\ f \oplus g \leq c}} \int_{\mathcal{X}} f(x) d\mu(x) + \int_{\mathcal{X}} g(y) d\nu(y), \quad (\text{dual}) \\ &= \max_{g \in C(\mathcal{X})} \int_{\mathcal{X}} g^c(x) d\mu(x) + \int_{\mathcal{X}} g(y) d\nu(y), \quad (\text{semi-dual}) \end{aligned}$$

where  $c(x, y) = \|x - y\|_2^2$ ,  $C(\mathcal{X})$  denotes continuous functions on  $\mathcal{X}$ , and  $g^c(x) := \min_{y \in \mathcal{X}} \{c(x, y) - g(y)\}$  is the  $c$ -transform of  $g$ . Given empirical probability measures (histograms)

$$\mu = \sum_{n=1}^{N_\mu} \alpha_n \delta_{y_n^\mu}, \quad \sum_{n=1}^{N_\mu} \alpha_n = 1, \quad \nu = \sum_{n=1}^{N_\nu} \beta_n \delta_{y_n^\nu}, \quad \sum_{n=1}^{N_\nu} \beta_n = 1,$$

the discretized semi-dual problem [11] is

$$\max_{g \in \mathbb{R}^{N_\mu}} \sum_{n=1}^{N_\mu} g^c(x_n) \alpha_n + \sum_{n=1}^{N_\nu} g(y_n) \beta_n, \quad (15)$$

where  $g^c(x_n) := \min_{q \in [N_\nu]} \{c(x_n, y_q) - g(y_q)\}$ .

Firstly, we derive that the Wasserstein barycenter defined in Eq. (11) has the dual formulation as presented in Eq. (13) when we consider its empirical estimation. In practical, the  $\hat{\mathcal{P}}(Y^1), \dots, \hat{\mathcal{P}}(Y^K)$  are given in the form of  $K$  sample-based empirical probability measures supported on a compact subset  $\mathcal{X} \subset \mathbb{R}^d$  with  $d \geq 1$ ,

$$\hat{\mathcal{P}}(Y^i) = \frac{1}{N_i} \sum_{n=1}^{N_i} \delta_{y_n^i}. \quad (16)$$

For multi-dimensional barycenter estimation, we follow prior research [11, 28, 36] to employ fixed-point iterations for computing empirical Wasserstein barycenter in given fix support  $\{\bar{y}_q\}_{q=1}^{\hat{N}}$  as an approximation to the unknown true Wasserstein barycenter distribution. The empirical Wasserstein barycenter can be estimated by

$$\hat{\mathcal{P}}^* = \sum_{n=1}^{\hat{N}} \alpha_n \delta_{\bar{y}_n}, \quad \sum_{n=1}^{\hat{N}} \alpha_n = 1, \alpha_n \geq 0. \quad (17)$$

Denoting the sample-based distributions  $\hat{\mathcal{P}}(Y^i)$  by  $\hat{\mathcal{P}}^i$ , with  $\mathcal{M}_1^+(\mathcal{X})$  presenting the set of all probability measures on  $\mathcal{X}$ , the semi-dual

problem of penalized Wasserstein barycenter problem can be formulated as

$$\begin{aligned} & \min_{\hat{\mathcal{P}}^* \in \mathcal{M}_1^+(X)} \max_{g_1, \dots, g_K} H(\hat{\mathcal{P}}^*, \mathbf{g}) \\ &= \sum_{i=1}^K \lambda_i \int_X g_i^c(y) d\hat{\mathcal{P}}^i(y) + \int_X \sum_{i=1}^K \lambda_i g_i(y) d\hat{\mathcal{P}}^*(y) \\ & \quad + \tau \int_X \log\left(\frac{d\hat{\mathcal{P}}^*}{dy}\right) d\hat{\mathcal{P}}^*(y). \end{aligned}$$

Plugging in the empirical distributions  $\hat{\mathcal{P}}^*, \hat{\mathcal{P}}^i, i \in [K]$  represented by Eq. (16) and Eq. (17), we obtain the empirical penalized Wasserstein barycenter problem

$$\begin{aligned} & \min_{\alpha_1, \dots, \alpha_{\hat{N}} \geq 0} \max_{g_1, \dots, g_K} \hat{H}(\alpha, \mathbf{g}) \\ & \quad \sum_{n=1}^{\hat{N}} \alpha_n = 1 \\ &= \sum_{i=1}^K \lambda_i \frac{1}{N_i} \sum_{n=1}^{N_i} g_i^c(y_n^i) + \sum_{n=1}^{\hat{N}} \sum_{i=1}^K \lambda_i g_i(\bar{y}_n) \alpha_n \quad (18) \\ & \quad + \tau \sum_{n=1}^{\hat{N}} \alpha_n \log(\alpha_n), \end{aligned}$$

where  $g_i^c(y_n^i)$  is defined by  $\min_{p=1, \dots, \hat{N}} \{\|y_n^i - \bar{y}_p\|_2^2 - g_i(\bar{y}_p)\}$ . It is explicit that Eq. (18) is concave to  $\alpha$  and convex to  $\mathbf{g}$ . Since the domain of  $\alpha$  is convex and compact, and the domains of  $g_i$ 's are convex, we can switch min and max according to Sion's minimax theorem,

$$\max_{g_1, \dots, g_K} \min_{\alpha_1, \dots, \alpha_{\hat{N}} \geq 0} \hat{H}(\alpha, \mathbf{g}). \quad (19)$$

The next step is to solve the inner minimum problem with respect to  $\alpha$  in Eq. (19). Introducing Lagrangian multiplier  $\kappa$  and  $\rho = (\rho_1, \dots, \rho_{\hat{N}})$ , we investigate the Lagrangian form,

$$\begin{aligned} & L(\alpha, \kappa, \rho) \\ &= \sum_{n=1}^{\hat{N}} \left( \sum_{i=1}^K \lambda_i g_i(\bar{y}_n) + \tau \log(\alpha_n) \right) \alpha_n + \kappa \left( \sum_{n=1}^{\hat{N}} \alpha_n - 1 \right) \quad (20) \\ & \quad - \sum_{n=1}^{\hat{N}} \rho_n \alpha_n. \end{aligned}$$

By Karush-Kuhn-Tucker (KKT) condition, for optimal solution  $(\alpha^*, \kappa^*, \rho^*)$ , we have

$$\begin{aligned} & \frac{\partial L}{\partial \alpha_n^*} = \sum_{i=1}^K \lambda_i g_i(\bar{y}_n) + \tau (\log(\alpha_n^*) + 1) + \kappa^* - \rho_n^* = 0, \\ & \rho_n^* \alpha_n^* = 0, \rho_n^* \geq 0, \quad n \in [\hat{N}], \\ & \left( \sum_{n=1}^{\hat{N}} \alpha_n^* - 1 \right) = 0. \end{aligned}$$

Solving these equations, the optimal solution  $\alpha^*$  can be formulated as

$$\alpha_n^* = \frac{\exp\left(-\frac{c_n}{\tau}\right)}{\sum_{q=1}^{\hat{N}} \exp\left(-\frac{c_q}{\tau}\right)}, \quad c_n = \sum_{i=1}^K \lambda_i g_i(\bar{y}_n). \quad (21)$$

Plugging Eq. (21) into Eq. (19), the empirical penalized Wasserstein barycenter problem turn to

$$\begin{aligned} \hat{H}(\alpha^*(\mathbf{g}), \mathbf{g}) &= \sum_{n=1}^{\hat{N}} \left( \sum_{i=1}^K \lambda_i g_i(\bar{y}_n) + \tau \log(\alpha_n^*) \right) \alpha_n^* \\ & \quad + \sum_{i=1}^K \lambda_i \frac{1}{N_i} \sum_{n=1}^{N_i} g_i^c(y_n^i) \\ &= \sum_{n=1}^{\hat{N}} -\tau \log \left( \sum_{n=1}^{\hat{N}} \exp \left( -\frac{1}{\tau} \sum_{i=1}^K \lambda_i g_i(\bar{y}_n) \right) \right) \alpha_n^* \\ & \quad + \sum_{i=1}^K \lambda_i \frac{1}{N_i} \sum_{n=1}^{N_i} g_i^c(y_n^i) \\ &= -\tau \log \left( \sum_{n=1}^{\hat{N}} \exp \left( -\frac{1}{\tau} \sum_{i=1}^K \lambda_i g_i(\bar{y}_n) \right) \right) \\ & \quad + \sum_{i=1}^K \lambda_i \frac{1}{N_i} \sum_{n=1}^{N_i} g_i^c(y_n^i). \end{aligned}$$

Consequently, we derive the dual problem of penalized Wasserstein barycenter as presented in Eq. (13). After we solve  $\max_{g_1, \dots, g_K} \hat{H}(\alpha^*(\mathbf{g}), \mathbf{g})$ , the empirical barycenter  $\hat{\mathcal{P}}^*$  can be recovered from  $\mathbf{g}$  by implementing Eq. (21). Then the optimal couplings  $\{T_i^*\}_{i=1}^K$  are able to be computed.

Next, we prove that  $\hat{H}(\alpha^*(\mathbf{g}), \mathbf{g})$  is concave with respect to  $\mathbf{g} = (g_i)_{i=1}^K$ . Let  $\hat{H}(\alpha^*(\mathbf{g}), \mathbf{g}) = F(\mathbf{g}) + G(\mathbf{g})$ ,

$$\begin{aligned} F(\mathbf{g}) &= -\tau \log \left( \sum_{n=1}^{\hat{N}} \exp \left( -\frac{1}{\tau} \sum_{i=1}^K \lambda_i g_i(\bar{y}_n) \right) \right), \\ G(\mathbf{g}) &= \sum_{i=1}^K \lambda_i \frac{1}{N_i} \sum_{n=1}^{N_i} g_i^c(y_n^i). \end{aligned}$$

For  $F(\mathbf{g})$ , log-sum-exp function is a classical convex function, and inside the log-sum-exp function is a linear combination which monotonically non-increasing in each component. The composition of the log-sum-exp function and the linear function here remains a convex function. Since the convex function multiplied by a negative constant is concave,  $F(\mathbf{g})$  is concave function to  $\mathbf{g}$ . For  $G(\mathbf{g})$ , note that  $g_i^c(y_n^i) = \min_{p=1, \dots, \hat{N}} \{\|y_n^i - \bar{y}_p\|_2^2 - g_i(\bar{y}_p)\}$ ,  $g_i^c(y_n^i)$  is concave to  $\mathbf{g}$  due to the fact that the min operation preserves concavity. It is explicit that  $G$  is concave, because  $G(\mathbf{g})$  is a linear combination of  $g_i^c(y_n^i)$ . Consequently,  $\hat{H}(\alpha^*(\mathbf{g}), \mathbf{g}) = F(\mathbf{g}) + G(\mathbf{g})$  is concave with respect to  $\mathbf{g}$ . Additionally, the dual problem can be reformulated as a convex optimization problem by considering  $\min_{g_1, \dots, g_K} -\hat{H}(\alpha^*(\mathbf{g}), \mathbf{g})$ .

## A.2 Numerical Optimization Scheme

Since we have established that the dual form Eq. (13) of the empirical penalized Wasserstein barycenter problem can be reformulated into an unconstrained convex optimization problem. Subgradient descent can be employed to solve for the optimal  $\mathbf{g}$ .

## A.3 Proof of Lemma 2

Given empirical distributions  $\hat{\mathcal{P}}(Y^i)$  and  $\hat{\mathcal{P}}^*$  with fix supports  $\{y_p^i\}_{p=1}^{N_i}$  and  $\{\bar{y}_q\}_{q=1}^{\bar{N}}$ . The optimal couplings  $T_i^*$  between  $\hat{\mathcal{P}}(Y^i)$  and  $\hat{\mathcal{P}}^*$  can be calculated with fixed input histograms. In this paper,  $\{y_p^i\}_{p=1}^{N_i}$  represents the embedding features of sample  $x_n^i$  extracted with model  $f(\theta)$ . The embedding distributions can be written as

$$\hat{\mathcal{P}}_\theta(Y^i) = \frac{1}{N_i} \sum_{n=1}^{N_i} \delta_{y_n^i(\theta)}, i \in [K]. \quad (22)$$

Hence, given the barycenter defined in the 2-Wasserstein distance problem turn to

$$\mathcal{W}_2^2(\hat{\mathcal{P}}_\theta(Y^i), \hat{\mathcal{P}}^*) = \min_{T_i \in U(1_{N_i}/N_i, \alpha)} \left\{ \sum_{p=1}^{N_i} \sum_{q=1}^{\bar{N}} T_i(p, q) c(y_p^i(\theta), \bar{y}_q) \right\}, \quad (23)$$

where  $c(y_p^i(\theta), \bar{y}_q) = \|y_p^i(\theta) - \bar{y}_q\|^2$  and  $U(1_{N_i}/N_i, \alpha)$  denotes that  $\{T(p, q) : \sum_{p=1}^{N_i} T(p, q) = \alpha, \sum_{q=1}^{\bar{N}} T(p, q) = 1/N_i\}$ . By envelope theorem [44],

$$\nabla_\theta \mathcal{W}_2^2(\hat{\mathcal{P}}_\theta(Y^i), \hat{\mathcal{P}}^*) = \sum_{p=1}^{N_i} \sum_{q=1}^{\bar{N}} T_i^*(p, q) \nabla_\theta c(y_p^i(\theta), \bar{y}_q). \quad (24)$$

Here,  $T^*$  is the transport plan that minimizes the objective in Equation (23). Similar techniques have been adopted in existing work (Lemma 1 of [53], Theorem 3 of [3]) to derive the gradient of the Wasserstein distance. Given 2-Wasserstein distance, using the chain rule, the gradient in (24) can be formulated as

$$\nabla_\theta \mathcal{W}_2^2(\hat{\mathcal{P}}_\theta(Y^i), \hat{\mathcal{P}}^*) \quad (25)$$

$$= \sum_{p=1}^{N_i} 2 \left[ \partial y_p^i(\theta) \right]^\top \left( \sum_{q=1}^{\bar{N}} T_i^*(p, q) (y_p^i(\theta) - \bar{y}_q) \right)_{p=1}^{N_i} \quad (26)$$

$$= \sum_{p=1}^{N_i} 2 \left[ \partial y_p^i(\theta) \right]^\top \left( \frac{y_p^i}{N_i} - \sum_{q=1}^{\bar{N}} T_i^*(p, q) \bar{y}_q \right)_{p=1}^{N_i}. \quad (27)$$

Plugging the gradient of 2-Wasserstein distance into (12), we get the representation in Lemma 2.

## B EXPERIMENTAL SETTINGS

### B.1 Dataset Pre-processing

For all used datasets, we first filter out users without valid attribute information. Following the settings described in previous studies [27, 57], for ML-1M, LFM-2B, and KuaiSAR, we retain only users with at least 5 interactions and items receiving at least 5 interactions from distinct users. For Last.fm-360K, we retain users with at

least 45 interactions and items receiving more than 45 interactions from distinct users. The characteristics of these datasets are summarized in Table 1. To evaluate recommendation performance, we use the widely employed leave-one-out testing [27], where we retain the last two items for each user (sorted by interaction time), using one as a validation item and the other as a test item. Regarding attribute data, we utilize two attributes from MovieLens, LFM-2B, and Last.fm-360K datasets: age and gender. Based on the previous studies [47, 57], we categorize the age attribute into three groups: above 45 years, below 35 years, and between 35 to 45 years, while the provided gender attribute is limited to female and male. For KuaiSAR, we utilize encrypted one-hot anonymous categories of users as the target attributes. In each dataset, we randomly sample 90% of the interaction data to serve as *the training set*, with the remaining 10% set aside as *the testing set*, which is not used during training.

## B.2 Parameter Settings

Our detailed experimental setup is as follows:

- **Recommendation Models:** All model parameters are initialized with a Gaussian distribution  $\mathcal{N}(0, 0.01^2)$ . To obtain the optimal performance, we use grid search to tune the hyper-parameters. For model-specific hyper-parameters, we follow the suggestions from their original papers. Specifically, we employ the SGD optimizer with a learning rate of  $1e-4$  and an embedding size of 32. The number of epochs is set to 10 for DMF, 20 for NCF, and 200 for LightGCN. For negative sampling, following prior work, we sample four items per iteration that the user has not interacted with, generating four negative samples for each positive interaction. Furthermore, for our RAID framework, we set the penalty coefficient  $\eta = 1$ , with the number of optimization rounds for the first and second phases set at 5 and 15, respectively. The frequency  $\xi$  of computing the central distribution is set at 4 and the penalty coefficient  $\tau$  for the centroids is set to 1.
- **Attacker:** For RF, we set the `n_estimators` to 100 and the `max_depth` to 20. For GBDT, we set the `n_estimators` to 100. All these three models are implemented with `scikit-learn 1.1.3`<sup>5</sup>. For XGBoost, we use the `xgboost` package<sup>6</sup>, setting the hyper-parameters as their default values. For AdaBoost, we set the `n_estimators` to 50. For MLP, we set the dimension of its hidden layer to 100, with a softmax layer serving as its output layer. Additionally, we set the L2 regularization weight to 1.0, the initial learning rate to  $1e-3$ , and the maximal iteration to 500, leaving the other hyper-parameters at their defaults.

## C MORE DISCUSSIONS

### C.1 Defend Against Attacks on Multiple Attributes

In real-world scenarios, attackers may target multiple sensitive attributes simultaneously. To evaluate RAID's capability to defend against multiple attribute attacks, we compare it with other baselines. For evaluation, we implement three unlearning strategies on the NCF model with the ML-1M dataset: i) AU-PoT and

<sup>5</sup><https://scikit-learn.org/>

<sup>6</sup><https://github.com/dmlc/xgboost/tree/stable>

RAID employ sequential attribute unlearning, ii) Adv-InT (also known as AdvX) implements simultaneous multi-attribute unlearning through adversarial training with multiple discriminators [13]. We then assess both recommendation performance and defense capability against multi-attribute attacks. The experimental results, as shown in Table 11, indicate the following observations: i) RAID achieves the lowest F1 and BAcc scores against two-attribute attacks compared to other methods; ii) Both RAID and AU-PoT maintain recommendation performance (HR/NDCG), with only marginal degradation when sequentially unlearning Age followed by Gender. These results demonstrate RAID’s effectiveness in protecting against multi-attribute attacks while preserving recommendation performance.

## C.2 Limitations and Future Work

Given the similarities between recommender system models and those used in social networks and mobile devices, our method can be straightforwardly extended to these domains. However, it is important to note that our assumptions regarding the attacker in recommender systems have certain limitations. We assume that the attacker can access the model’s parameters or the outcomes of the recommendations, rather than the original training data. This assumption may have restrictions in real-world scenarios, and future research could further explore this aspect of the attack model. Additionally, our method currently only handles attributes that are discrete variables and cannot manage continuous variable attributes that have not been discretized. Addressing more general vector attributes is also a direction worthy of improvement in future research.

**Table 11: Results of recommendation performance and attribute inference attack on defending against attacks on multiple attributes. The top results are highlighted in bold.**

Attribute	Method	HR@10	NDCG@10	F1	BAcc
Gender	Original	0.1040	0.0520	0.7501	0.7487
	DP-PoT	0.0490	0.0240	0.4425	<b>0.4425</b>
	AU-PoT	<b>0.1000</b>	<b>0.0510</b>	0.4868	0.4910
	Adv-InT	0.0970	0.0490	0.6180	0.6106
	RAID	0.0890	0.0460	<b>0.2666</b>	0.5000
Gender, Age	Original	0.0820	0.0410	0.7162	0.7188
	DP-PoT	0.0220	0.0097	0.4777	0.4776
	AU-PoT	<b>0.0840</b>	<b>0.0417</b>	0.4895	0.4345
	Adv-InT	0.0833	0.0410	0.4962	0.4665
	RAID	0.0835	0.0410	<b>0.4368</b>	<b>0.4334</b>

## D MORE EMPIRICAL RESULTS

*Recommendation Performance.* To verify the effectiveness of the RAID framework in maintaining recommendation performance, we employ NDCG and HR for evaluation, truncating the ranking lists at 5, 10, 15, and 20. We report the results of the ranking lists at 15 and 20 in Table 12.

*Efficiency.* Compared to other InT methods, such as Adv-InT, our method exhibits significant efficiency improvements. Under the conditions of maintaining the same learning rate and setting an early stopping strategy, i.e., terminating training when the sum

of defense loss and recommendation loss convergence, we conduct a comparison of all unlearning methods across each dataset and model. We report the running times in Figure 6. From it, we observe that our proposed RAID significantly outperforms Adv-InT in terms of efficiency and stability. This is primarily because Adv-InT tends to be unstable during training, prone to fluctuations, and thus difficult to converge. In contrast, our method is more stable during parameter updates.

**Table 12: Results of recommendation performance with truncating the ranking list for these metrics at 15 and 20. The top results are highlighted in bold.**

Dataset	Attribute	Method	DMF				NCF				LightGCN			
			HR@15	NDCG@15	HR@20	NDCG@20	HR@15	NDCG@15	HR@20	NDCG@20	HR@15	NDCG@15	HR@20	NDCG@20
ML-1M	Gender	Original	0.1390	0.0620	0.1670	0.0680	0.1430	0.0640	0.1730	0.0710	0.1310	0.0580	0.1590	0.0580
		DP-PoT	0.0630	0.0270	0.0790	0.0310	0.0240	0.0090	0.0310	0.0110	0.0560	0.0260	0.0640	0.0270
		AU-PoT	<b>0.1340</b>	<b>0.0590</b>	<b>0.1630</b>	<b>0.0660</b>	0.1080	0.0490	0.1350	0.0560	0.1040	0.0480	0.1280	0.0540
		RAID	0.1230	0.0540	0.1470	0.0600	<b>0.1310</b>	<b>0.0560</b>	0.1600	<b>0.0630</b>	<b>0.1160</b>	<b>0.0520</b>	<b>0.1450</b>	<b>0.0580</b>
	Age	Original	0.1390	0.0620	0.1670	0.0680	0.1430	0.0640	0.1730	0.0710	0.1310	0.0580	0.1590	0.0580
		DP-PoT	0.0600	0.0240	0.0750	0.0280	0.0240	0.0090	0.0310	0.0110	0.0560	0.0250	0.0650	0.0270
		AU-PoT	0.1150	0.0510	0.1470	0.0590	0.1250	0.0570	0.1550	0.0640	0.1040	0.0480	0.1270	0.0530
		RAID	<b>0.1200</b>	<b>0.0530</b>	<b>0.1490</b>	<b>0.0600</b>	<b>0.1330</b>	<b>0.0600</b>	<b>0.1640</b>	<b>0.0680</b>	<b>0.1210</b>	<b>0.0540</b>	<b>0.1540</b>	<b>0.0610</b>
LFM-2B	Gender	Original	0.0270	0.0110	0.0330	0.0130	0.0370	0.0160	0.0470	0.0190	0.0440	0.0210	0.0520	0.0230
		DP-PoT	0.0070	0.0030	0.0080	0.0030	0.0030	0.0010	0.0050	0.0020	0.0080	0.0030	0.0090	0.0040
		AU-PoT	0.0120	0.0050	0.0160	0.0060	0.0280	0.0120	0.0330	0.0130	0.0400	<b>0.0190</b>	0.0490	<b>0.0210</b>
		RAID	<b>0.0240</b>	<b>0.0100</b>	<b>0.0290</b>	<b>0.0110</b>	<b>0.0310</b>	<b>0.0140</b>	<b>0.0370</b>	<b>0.0160</b>	<b>0.0420</b>	0.0180	<b>0.0500</b>	0.0200
	Age	Original	0.0270	0.0110	0.0330	0.0130	0.0370	0.0160	0.0470	0.0190	0.0440	0.0210	0.0520	0.0230
		DP-PoT	0.0060	0.0020	0.0080	0.0030	0.0030	0.0010	0.0050	0.0020	0.0070	0.0030	0.0090	0.0040
		AU-PoT	0.0210	0.0090	<b>0.0280</b>	0.0090	0.0280	0.0120	0.0340	0.0140	<b>0.0410</b>	<b>0.0190</b>	<b>0.0490</b>	<b>0.0210</b>
		RAID	<b>0.0240</b>	<b>0.0110</b>	<b>0.0280</b>	<b>0.0120</b>	<b>0.0340</b>	<b>0.0160</b>	<b>0.0400</b>	<b>0.0180</b>	0.0390	0.0170	0.0480	0.0200
KuaiSAR	Gender	Original	0.0410	0.0180	0.0480	0.0200	0.0430	0.0180	0.0520	0.0200	0.0500	0.0210	0.0610	0.0240
		DP-PoT	0.0090	0.0040	0.0130	0.0050	0.0070	0.0030	0.0090	0.0030	0.0160	0.0070	0.0200	0.0080
		AU-PoT	0.0380	0.0160	0.0490	0.0190	<b>0.0390</b>	<b>0.0180</b>	<b>0.0490</b>	<b>0.0200</b>	0.0430	0.0190	0.0530	0.0210
		RAID	<b>0.0430</b>	<b>0.0190</b>	<b>0.0550</b>	<b>0.0220</b>	<b>0.0390</b>	<b>0.0180</b>	<b>0.0490</b>	<b>0.0200</b>	<b>0.0470</b>	<b>0.0200</b>	<b>0.0580</b>	<b>0.0220</b>
	Age	Original	0.0400	0.0170	0.0500	0.0200	0.0430	0.0180	0.0520	0.0200	0.0500	0.0210	0.0610	0.0240
		DP-PoT	0.0090	0.0030	0.0110	0.0040	0.0070	0.0030	0.0090	0.0030	0.0160	0.0060	0.0190	0.0070
		AU-PoT	<b>0.0360</b>	<b>0.0150</b>	0.0460	<b>0.0180</b>	<b>0.0390</b>	<b>0.0170</b>	<b>0.0500</b>	<b>0.0200</b>	0.0410	0.0170	0.0500	0.0200
		RAID	<b>0.0360</b>	<b>0.0150</b>	<b>0.0470</b>	<b>0.0180</b>	0.0380	0.0160	<b>0.0500</b>	0.0190	<b>0.0440</b>	<b>0.0200</b>	<b>0.0560</b>	<b>0.0230</b>
Last.fm-360K	Gender	Original	0.1390	0.0620	0.1690	0.0690	0.1420	0.0640	0.1720	0.0710	0.1470	0.0660	0.1780	0.0730
		DP-PoT	0.1200	0.0520	0.1460	0.0590	0.1170	0.0510	0.1430	0.0570	0.0410	0.0180	0.0500	0.0200
		AU-PoT	<b>0.1390</b>	<b>0.0620</b>	<b>0.1690</b>	<b>0.0690</b>	<b>0.1420</b>	<b>0.0640</b>	<b>0.1720</b>	<b>0.0710</b>	<b>0.1470</b>	<b>0.0660</b>	<b>0.1780</b>	<b>0.0730</b>
		RAID	<b>0.1390</b>	<b>0.0620</b>	<b>0.1690</b>	<b>0.0690</b>	0.1380	0.0620	0.1680	0.0690	<b>0.1470</b>	<b>0.0660</b>	<b>0.1780</b>	<b>0.0730</b>
	Age	Original	0.1390	0.0620	0.1690	0.0690	0.1420	0.0640	0.1720	0.0710	0.1470	0.0660	0.1780	0.0730
		DP-PoT	0.1200	0.0520	0.1460	0.0590	0.1170	0.0510	0.1430	0.0570	0.0410	0.0180	0.0500	0.0200
		AU-PoT	<b>0.1390</b>	<b>0.0620</b>	<b>0.1690</b>	<b>0.0690</b>	<b>0.1420</b>	<b>0.0640</b>	<b>0.1720</b>	<b>0.0710</b>	<b>0.1470</b>	<b>0.0660</b>	<b>0.1780</b>	<b>0.0730</b>
		RAID	0.1340	0.0590	0.1630	0.0660	0.1320	0.0570	0.1610	0.0640	0.1360	0.0620	0.1660	0.0690

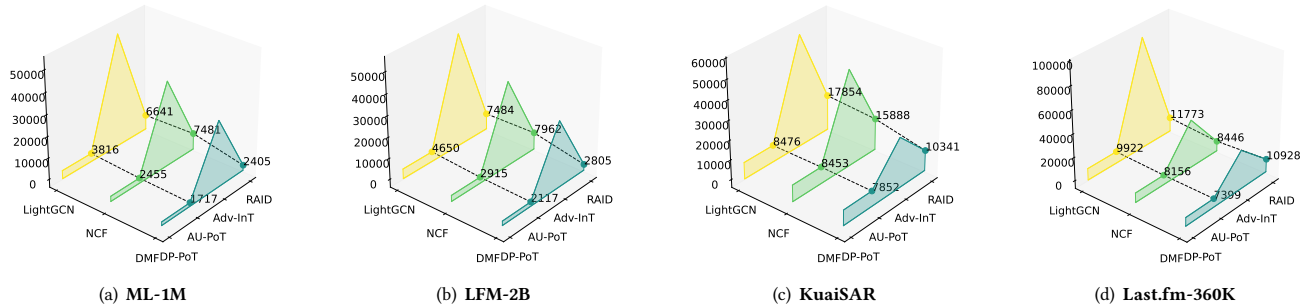


**Figure 6: Running time of unlearning methods.**